

# We are IntechOpen, the world's leading publisher of Open Access books Built by scientists, for scientists

4,800

Open access books available

122,000

International authors and editors

135M

Downloads

Our authors are among the

154

Countries delivered to

TOP 1%

most cited scientists

12.2%

Contributors from top 500 universities



WEB OF SCIENCE™

Selection of our books indexed in the Book Citation Index  
in Web of Science™ Core Collection (BKCI)

Interested in publishing with us?  
Contact [book.department@intechopen.com](mailto:book.department@intechopen.com)

Numbers displayed above are based on latest data collected.  
For more information visit [www.intechopen.com](http://www.intechopen.com)



---

# Hydrogen Conversion in DC and Impulse Plasma-Liquid Systems

---

Valeriy Chernyak, Oleg Nedybaliuk, Sergei Sidoruk,  
Vitalij Yukhymenko, Eugen Martysh,  
Olena Solomenko, Yulia Veremij, Dmitry Levko,  
Alexandr Tsimbaliuk, Leonid Simonchik,  
Andrej Kirilov, Oleg Fedorovich, Anatolij Liptuga,  
Valentina Demchina and Semen Dragnev

Additional information is available at the end of the chapter

<http://dx.doi.org/10.5772/53764>

---

## 1. Introduction

It is well known [1] that hydrogen (H<sub>2</sub>) as the environmentally friendly fuel is considered to be one of the future most promising energy sources. Recently, interest in hydrogen energy has increased significantly, mainly due to the energy consumption increase in the world, and recent advances in the fuel cell technology. According to the prognosis, in the next decades, global energy consumption will be increased by 59%, and still most of this energy will be extracted from the fossil fuels. Because of the traditional fossil fuels depletion, today there's a growing interest in renewable energy sources (f.e. – bioethanol, biodiesel). Bioethanol can be obtained from the renewable biomass, also it can be easily and safely transported due to its low toxicity, but it's not a very good fuel. Modern biodiesel production technologies are characterized by a high percentage of waste (bioglycerol) which is hard to recycle.

It is common knowledge [2] that addition of the syn-gas to the fuel (H<sub>2</sub> and CO) improves the combustion efficiency: less burning time, rapid propagation of the combustion wave, burning stabilization, more complete mixture combustion and reduction of dangerous emissions (NO<sub>x</sub>). Besides, the synthesis gas is an important stuff raw for the various materials and synthetic fuels synthesizing. There are many methods of synthesis gas (including hydrogen) production, for example – steam reforming and partial liquid hydrocarbons oxidation. Also,

there is an alternative approach – biomass reforming with low-temperature plasma assistance. Plasma is a very powerful source of active particles (electrons, ions, radicals, etc.), and therewith it can be catalyst for the various chemical processes activation. However, a major disadvantage of chemical processes plasma catalysis is weak processes control.

There is a bundle of electrical discharges that generate both equilibrium and non equilibrium plasma. For plasma conversion – arc, corona, spark, microwave, radio frequency, barrier and other discharges are used. One of the most effective discharges for the liquid hydrocarbons plasma treatment is the "tornado" type reverse vortical gas flow plasma-liquid system with a liquid electrode ("TORNADO-LE") [3]. The main advantages of plasma-liquid systems are – high chemical plasma activity and good plasma-chemical conversions selectivity. It may guarantee high performance and conversion efficiency at the relatively low power consumption. Moreover, those are systems of atmospheric pressure and above, and this increases their technological advantages.

Also, syn-gas ratio – hydrogen and carbon monoxide concentration ratio should be mentioned. As well, it should be taken into consideration that for efficient combustion (in terms of energy) of the synthesis gas it should contain more hydrogen, and in the case of the synthesis materials – they should contain more CO.

Relatively new possible solution to this problem – carbon dioxide recycling. Many modern energy projects have difficulties with the large amount of CO<sub>2</sub> storing and disposing. And it is also known that the addition of CO<sub>2</sub> to plasma during the hydrocarbons reforming may help to control plasma-chemical processes [4]. That is why the objective of the research is to study the influence of different amounts of CO<sub>2</sub> in the working gas on the plasma-chemical processes during the hydrocarbons conversion.

This research deals with hydrocarbons (bioethanol, bioglycerol) reforming by means of the combined system, which includes plasma processing and pyrolysis chamber. As a plasma source the "tornado" type reverse vortical gas flow plasma-liquid system with liquid electrode has been used [5].

Qualitatively new challenge is connected with a selectivity of the plasma chemistry strengthening by the transition of the chemical industry to "green chemistry". The last is a transition from the traditional concept of evaluating the effectiveness of the chemical yield to the concept that evaluates the cost-effectiveness as the exclusion of hazardous waste and non-toxic and/or hazardous substances [6].

A quantitative measure of the environmental acceptability of chemical technology is the ecology factor, which is defined as the ratio of the mass of waste (waste) to the mass of principal product. Waste is all that is not the principal product.

By the way, the most promising approaches in green chemistry is the implementation of processes in supercritical liquids (water, carbon dioxide) [7].

Water in supercritical condition unlimitedly mixes with oxygen, hydrogen and hydrocarbons, facilitating their interaction with each other - oxidation reactions are very fast in scH<sub>2</sub>O (supercritical water). One particularly interesting application of this water - efficient destruc-

tion of chemical warfare agents. When mixed with other substances  $\text{scH}_2\text{O}$  can be used not only for oxidation but also in the reactions of hydrolysis, hydration, the formation and destruction of carbon-carbon bonds, hydrogenation, and others.

Besides, the use of pulsed electrical discharges in the liquid brings up new related factors: strong ultraviolet emission and acoustic or shock waves. In literature it can be found that systems with energies more than 1 kJ/pulse, that have negative influence on the lifetime of such systems. Reasonable from this perspective is the usage of pulsed systems with relatively low pulse energy and focusing of acoustic waves. In addition, the acoustic oscillations in such systems can be used as an additional mechanism of influence on chemical transformations.

In using of acoustic oscillations for chemical reactions the most attention is paid to systems with strong convergent waves. However, the processes during the collapse of the powerful convergent waves are studied insufficiently. In the literature the systems of cylindrical, spherical or parabolic surfaces used in the focusing of shock waves for technological needs are known [8]. However, among their disadvantages should be noted that partial usage of the energy of acoustic wave and the problem of its peripheral sources synchronization, which leads to distortion of the shock wave front ideality and reduces the focusing effectiveness.

Probably, more perspective method of using acoustic waves is their generation by single axial pulse electric discharge with further reflection from an ideal cylindrical surface. This approach can provide better symmetry of compression by convergent acoustic wave both in the gas and in the liquid. Probably, such mechanism can be exploited for  $\text{scH}_2\text{O}$  production

In addition, the re-ignition of electrical discharge at the moment of collapse convergent acoustic waves can lead to the plasma temperature increasing due to compression of the discharge channel, as well as the appropriate amplification of acoustic waves after the collapse.

It's clear that plasma-liquid systems (PLS) mentioned above have some sharp differences. Therefore, the first section of this article presents the results of our research on the addition of  $\text{CO}_2$  to the "TORNADO-LE". And the second section of the article is devoted to investigation of double-impulse system in underwater electric discharge.

## **2. Bioethanol and bioglycerol conversion in "tornado" type plasma-liquid system with the addition of $\text{CO}_2$**

### **2.1. Experimental set up**

The experimental setting is shown in Fig. 1. Its base is a cylindrical quartz chamber (1) with diameter of 90 mm and height of 50 mm. Top (2) and bottom (3) it is hermetically closed with metal flanges. Camera is filled with fluid (4), the level of which has been maintained by the injection pump through the hole (5). Bottom flange is made of stainless steel. The stainless steel T-shaped cylindrical electrode (6), cooled with water, immerses in the liquid through the central hole in the bottom flange. There is a 5 mm thick metal washer on its surface (7) in the middle of which there is a hole in diameter of 10 mm. Sharp corners are rounded. This washer

is used for reducing the waves (which have been moving to the quartz wall) amplitude on the liquid surface.

The top flange, made from duralumin, contains copper sleeve (13) with a diameter of 20 mm is placed in the center (2), and plays the role of the second electrode. The nozzle with diameter of 4 mm and length of 6 mm is located in the center of the copper sleeve (8). Gas is introduced into the flange (2) through the aperture (9). Gas flow changes the direction at 90 degrees inside the flange and injects tangentially into the channel (10). (10) The gas is rotated in the circular channel. Rotating gas (11) lands on the surface liquid and moves to the central axis of the system, where falls into the quartz cell through the nozzle (14), forming a plasma torch (12). Camera (14), in its turn, plays a role of pyrolytic chamber. Flow rate reaches the maximum value near the nozzle. Due to this, the zone of lower pressure is formed in the center of the gas layer, compared to the periphery. The conical structure appears over the liquid's surface near the system axis (Fig. 1). External static pressure is 1 atm. and internal - 1.2 atm (during discharge burning). Gas from quartz chamber (14) gets into the refrigerator (15), which is cooled with water at room temperature.

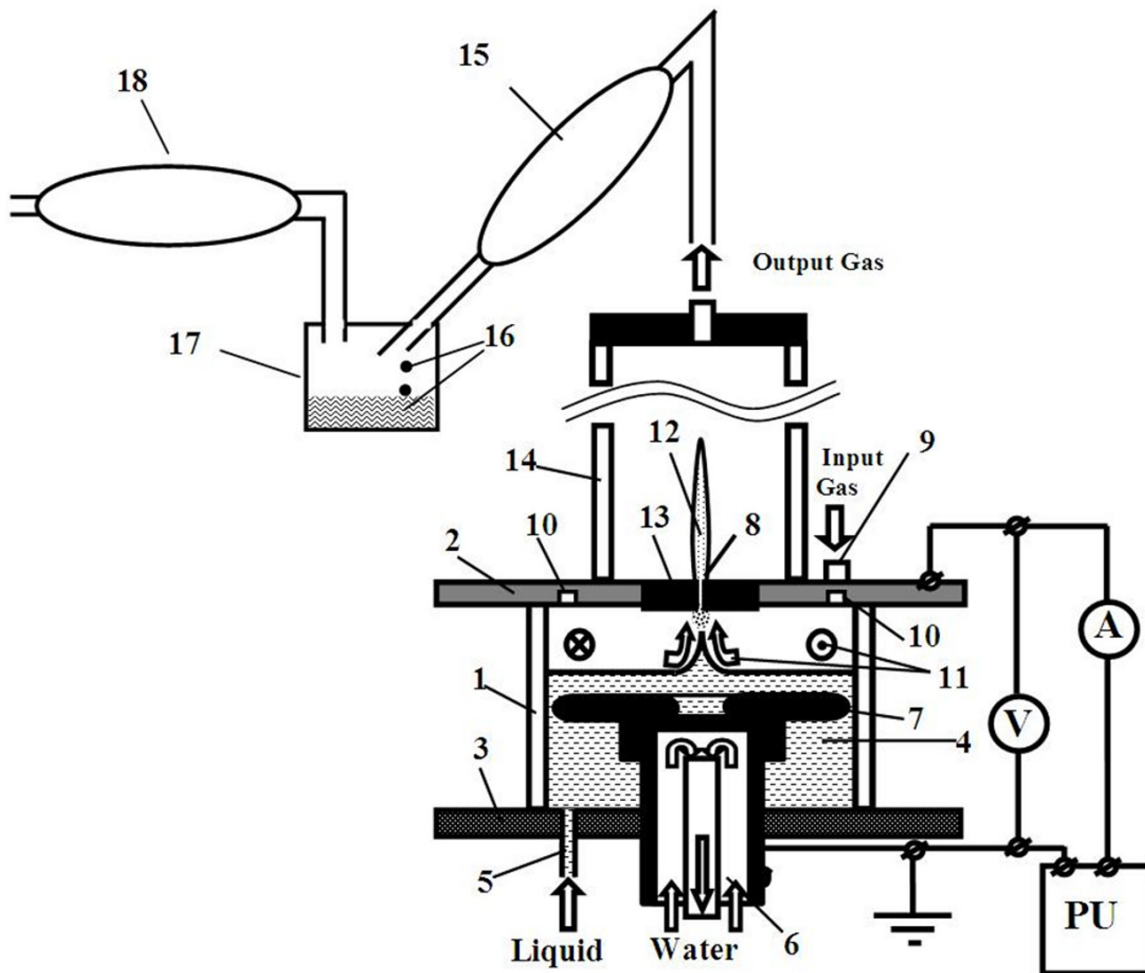


**Figure 1.** Schematic set up of the "TORNADO-LE".

Condensed matter (16) together with the gas from the refrigerator gets to the chamber (17). At the chamber exit (17) there's a flask (18), where gas is gathered for its composition diagnostics by means of mass spectrometry and gas chromatography. Study of plasma parameters is performed by emission spectrometry. The emission spectra registration procedure uses the system which consists of optical fiber, the spectral unit S-150-2-3648 USB, and the computer. Fiber is focusing on the sight line in the middle between the top flange (2) and the surface of the liquid (4).

The spectrometer works in the wavelength range from 200 to 1100 nm. The computer is used in both control measurements process and data processing, received from the spectrometer.

The voltage between the top flange and electrode, immersed in the liquid, is supplied by the power unit "PU". DC voltage provided is up to 7 kV. Two modes of operation have been considered:

1. "liquid" cathode (LC) – electrode immersed in the liquid has "minus" and the top flange has "plus";
2. "solid" cathode (SC) - with the opposite polarity.

Electrode which has "plus" is grounded. Breakdown conditions are controlled by three parameters: the fluid level, the gas flow value and the voltage magnitude between the electrodes. The several modes of operation have been studied:

1. Various air flow and CO<sub>2</sub> ratio;
2. Discharge voltage varied within  $U_d = 2.2 \div 2.4$  kV;
3. Discharge current varied within  $I_d = 220 \div 340$  mA (ballast resistance hasn't been used).

At first, for the analysis of the plasma-chemical processes kinetics the distilled water (working fluid), and ethanol (ethyl alcohol solution in distilled water with a molar ratio C<sub>2</sub>H<sub>5</sub>OH/H<sub>2</sub>O = 1/9.5), as a hydrocarbon model have been used. As the working gas mixture of air with CO<sub>2</sub>, in a wide range of air flow and CO<sub>2</sub> ratios has been used. The ratio between air and CO<sub>2</sub> in the working gas changes in the ranges: CO<sub>2</sub>/Air = 1/20 ÷ 1/3 for the working fluid C<sub>2</sub>H<sub>5</sub>OH/H<sub>2</sub>O (1/9.5) and CO<sub>2</sub>/Air = 0/1 ÷ 1/0 (by pure air to pure CO<sub>2</sub>) - for distilled water.

Plasma component composition and population temperature of the excited electron ( $T_e^*$ ), vibration ( $T_v^*$ ) and rotational ( $T_r^*$ ) levels of plasma components and relative concentrations of these components have been determined by the emission spectra. For the temperature population determination of the excited oxygen atoms electron levels the Boltzmann diagram method has been used [5].  $T_e^*$  of oxygen atoms has been determined for the three most intense lines (777.2 nm, 844 nm, 926 nm). Temperature population of excited hydrogen atoms electron levels has been determined by the two lines of 656.3 nm and 486 nm relative intensities.

The effect of the presence of CO<sub>2</sub> in the system on the initial gas products has been investigated by means of "TORNADO-LE" current-voltage characteristics with changes in the working gas composition.  $T_v^*$  and  $T_r^*$  have been determined by comparing the experimentally measured emission spectra with the molecules spectra simulated in the SPECAIR program [9]. With help

of this program and measured spectra, relative component concentrations in plasma have been determined. Also, the concentration of atomic components has been obtained by calculating the amount of oxygen that fell into a working system with the working gas flow. The hydrogen amount has been received from the electrolysis calculations. The output gas in reforming ethanol has been analyzed by gas chromatography and infrared absorption.

## 2.2. Results

The process of discharge ignition occurred as follows: the chamber is filled with liquid to a fixed level (5 mm above the washer). At the next stage a certain amount of gas flow forms the stationary cone from liquid; the voltage applied between the top flange and electrode immersed in a liquid starts gradually increase. When the voltage reaches a break-out value -  $U_b$ , a streamer appears for the first time. After that, burning discharge starts in split second, and then voltage decreases and current increases. After a second or two it is stabilized. During this time – static pressure rises inside the chamber from 1 to 1.2 atm. If you maintain the liquid level fixed, then the discharge is quite steady.

Liquid layer thickness of 5 mm has been chosen because that is the minimum liquid thickness in which the discharge burns between the liquid surface and the top flange. If the thickness is smaller plasma pushes the water toward the electrode immersed in the liquid and the discharge starts burning between two metal electrodes. Discharge goes into the arc regime. When the thickness of the distilled water layer above the washer is 5 mm (in the case of air flow only) break voltage reaches 4.5 kV and for a  $\text{CO}_2$  flow - 6 kV. It is known [10], this increase in break-out voltage derives from the appearance of an additional loss channel of electrons – due to their sticking onto  $\text{CO}_2$  molecules. This sticking has dissociative character and it is accompanied by the energy expense.

For example, the threshold reaction with  $\text{CO}_2$  is 3.85 eV. Therefore CVC in pure  $\text{CO}_2$  is decreased (Fig. 2). When the thickness of the  $\text{C}_2\text{H}_5\text{OH}/\text{H}_2\text{O}$  (1/9.5) solution layer above the washer is 5 mm (in the case of air flow only) the break voltage is 5.5 kV, and for the air flow mixture with  $\text{CO}_2$  ( $\text{CO}_2/\text{Air} = 1/3$ ) – 6.5 kV. Adding  $\text{CO}_2$  to the air leads to the increase in the break-out voltage value. Adding ethanol to distilled water ( $\text{C}_2\text{H}_5\text{OH}/\text{H}_2\text{O} = 1/9.5$ ) results in the increase of break voltage on 1 kV. Power supply unit provides maximum voltage of 7 kV. Increasing the thickness of the fluid layer above the washer (> 5 mm) leads to the increase of the break-out voltage value. There is no discharge ignition with a break-out voltage value of more than 7 kV. Therefore, 5 mm thickness of the liquid layer above the surface immersed in a liquid metal electrode (washer) has been chosen as the optimum one.

The current-voltage characteristics of the discharge are shown for the SC mode (Fig. 2 a; 2b). The cell has been filled with distilled water (Fig. 2a) or bioethanol (Fig. 2b).

The "tornado" type reverse vortex gas flow is formed by gas flow, which is a mixture of air with  $\text{CO}_2$  in varying proportions. Ratio of  $\text{CO}_2/\text{Air}$  is changed in the range from 1/20 to 1/3, and in the case of ethanol and 1/0 in the case of water. Current varied in the range from 230 to 400 mA. The initial level of the working liquid is the same in all cases.

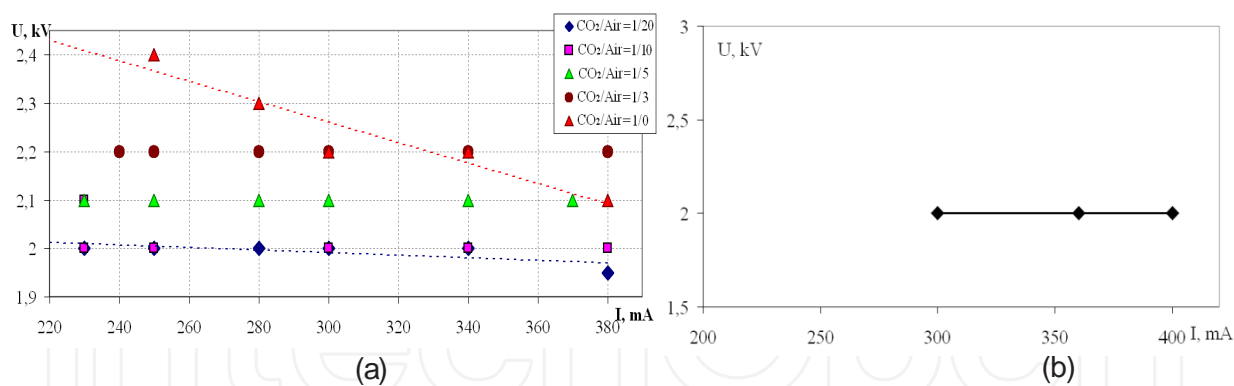


**Figure 2.** a) Current-voltage characteristics of the discharge at different ratios of CO<sub>2</sub>/Air in the working gas. Working liquid - distilled water. Airflow - 55 and 82.5 cm<sup>3</sup>/s, the flow of CO<sub>2</sub> - 4.25, 8.5 and 17 cm<sup>3</sup>/sec. b) Current-voltage characteristics of the discharge at the ratio CO<sub>2</sub>/Air = 1/5 in the working gas. Working liquid - C<sub>2</sub>H<sub>5</sub>OH/H<sub>2</sub>O (1/9.5) solution. Airflow - 82.5 cm<sup>3</sup>/s, the flow of CO<sub>2</sub> - 17 cm<sup>3</sup>/s.

The current-voltage characteristics show that adding a small amount of CO<sub>2</sub> (near 20%) to the working gas has no effect on the discharge type in various studied working liquids. In the range of flow ratios CO<sub>2</sub>/Air from 1/20 to 1/5 characteristics are straight lines. It was observed that the increasing of CO<sub>2</sub> share in working gas causes discharge voltage supply rise.

Typical emission spectra of the plasma are shown in Fig. 3a and Fig. 3b for the cases with the distilled water as the working liquid and the solution of C<sub>2</sub>H<sub>5</sub>OH/H<sub>2</sub>O (1/9.5).

The emission spectra show that when the working liquid is distilled water, plasma contains the following components: atoms H, O, and hydroxyl OH. In case when the working liquid is C<sub>2</sub>H<sub>5</sub>OH/H<sub>2</sub>O solution (1/9.5), plasma has the following components: atoms - N, O, C, Fe, Cr, molecules - OH, CN, NH. The emission spectra shows that the replacement of the working liquid with distilled water with ethanol CN and lower electrode material made of stainless steel (anode) occur in plasma. Occasionally, during discharge burning breakdown may occur in C<sub>2</sub>H<sub>5</sub>OH/H<sub>2</sub>O layer solution (1/9.5).

Those breakdowns may occur due to the fact that during the discharge burning, thickness of liquid layer, when the working fluid has a significant share of C<sub>2</sub>H<sub>5</sub>OH, a current channel is formed through the liquid layer to the metal electrode. And in the case of distilled water - plasma channel discharge ends near the surface of the liquid. It may indicate the presence of large liquid surface charge.

It was observed that the increase of CO<sub>2</sub> in the working gas (CO<sub>2</sub>/air > 0.3) leads to an increase in the intensity of hydrogen and oxygen radiation lines (H and O) at the time when the intensity of the molecular component (OH) radiation, within the error, is stable (I = 300 mA, U = 1.9-2.4 kV, air flow 0 - 82.5 cm<sup>3</sup>/sec, the flow of CO<sub>2</sub> - 4.25 - 85 cm<sup>3</sup>/sec).

Fig. 4 shows the ratio of the hydrogen (H $\alpha$   $\lambda$  = 656.3 nm) and oxygen (O,  $\lambda$  = 777.2 nm) radiation intensity to the highest point of band hydroxyl (OH,  $\lambda$  = 282.2 nm) small intensity at different ratios of CO<sub>2</sub>/air (I = 300 mA, U = 1.9 - 2.4 kV, air flow - 27.5, 55 and 82.5 cm<sup>3</sup>/s, the flow of CO<sub>2</sub> - 4.25, 8.5, 17, 42.5 and 85 cm<sup>3</sup>/s). High intensity bands haven't been used in the calculations because of the possible reabsorption. (I = 300 mA, U = 2 - 2.2 kV). In the case of distilled water



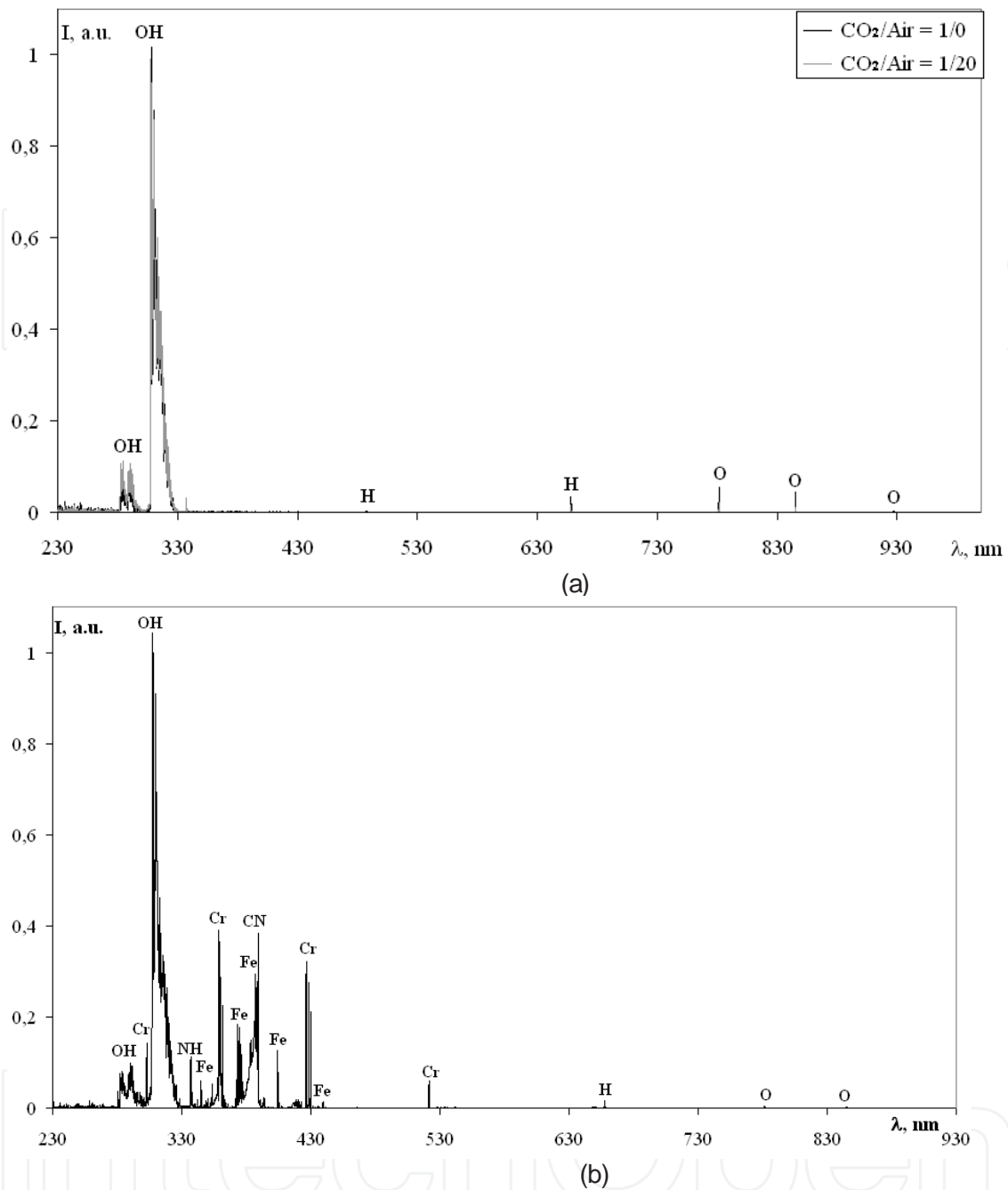


**Figure 3.** a) Emission spectrum of the plasma in TORNADO-LE plasma-liquid system, where the working liquid is distilled water. Working gas - a mixture of CO<sub>2</sub>/air = 1/0, I<sub>d</sub> = 300 mA, U = 2.2 kV, the flow of CO<sub>2</sub> - 85 cm<sup>3</sup>/s and CO<sub>2</sub>/air = 1/20, I<sub>d</sub> = 300 mA, U = 1.9 - 2.0 kV, air flow - 82.5 cm<sup>3</sup>/s, the flow of CO<sub>2</sub> - 4.25 cm<sup>3</sup>/s. b) Emission spectrum of the plasma in the TORNADO-LE plasma-liquid system, where the working liquid is bioethanol. Working gas - a mixture of CO<sub>2</sub>/air = 1/20, I<sub>d</sub> = 300 mA, U = 2 kV, air flow - 82.5 cm<sup>3</sup>/sec, the flow of CO<sub>2</sub> - 4.25 cm<sup>3</sup>/sec.

(Fig. 4a), results are presented for the three air flows - 27.5, 55 and 82.5 cm<sup>3</sup>/s and five CO<sub>2</sub> streams - 4.25, 8.5, 17, 42.5 and 85 cm<sup>3</sup>/s (I = 300 mA, U = 1.9 - 2.4 kV). Air and CO<sub>2</sub> flows are varied so that the total flow compiles similar values and achieves ratios of CO<sub>2</sub>/air in a wide range from 1/20 to 1/0.

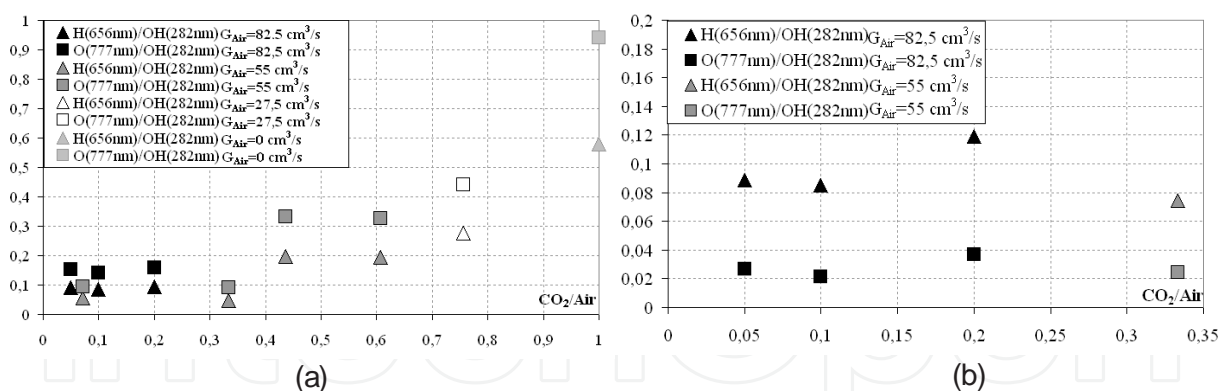


**Figure 4.** The ratio of the radiation intensity of hydrogen ( $H_{\alpha}$   $\lambda = 656.3$  nm) and oxygen (O,  $\lambda = 777.2$  nm) to the peak of the band hydroxyl (OH  $\lambda = 282,2$  nm) at different ratio  $CO_2/Air$  in the working gas. Working liquid - distilled water (a)  $I = 300$  mA,  $U = 1.9 - 2.4$  kV and bioethanol (b)  $I = 300$  mA,  $U = 2 - 2.2$  kV.

In calculating the relative concentration ratio of hydrogen to oxygen from the emission spectra, it was observed that the hydrogen concentration is two times as much of the oxygen concentration for the case of distilled water as the working liquid - ( $I = 300$  mA,  $U = 1.9 - 2.4$  kV, airflow - 27.5, 55 and 82.5  $cm^3/sec$ , the flow of  $CO_2$  - 4.25, 8.5, 17, 42.5 and 85  $cm^3/sec$ ), and ten times as much when the working liquid is  $C_2H_5OH/H_2O$  solution (1/9.5) ( $I = 300$  mA,  $U = 2 - 2.2$  kV, air flow - 55 and 82.5  $cm^3/sec$ , the flow of  $CO_2$  - 4.25, 8.5 and 17  $cm^3/sec$ ). However, according to the calculations, these components production by means of electrolysis and their extraction from the working gas, the oxygen concentration exceeds the average hydrogen concentration in three orders of magnitude, unless the case when the pure  $CO_2$  is used as a working gas.

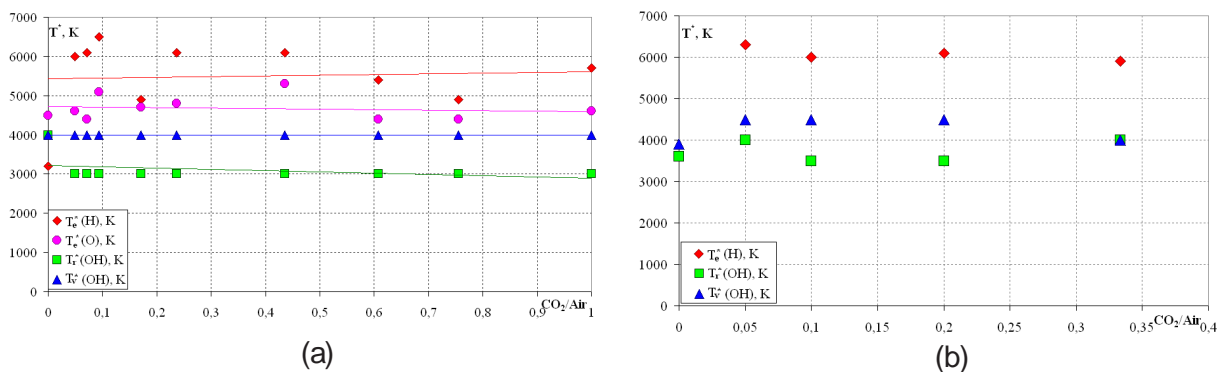
It should be noted that the addition of  $CO_2$  reduces the discharge stability, especially in the case of bioethanol. In determination of the temperature population excited electron levels of plasma atomic component the most intense lines (spectra with the smallest possible accumulation in the experiment measurement of 500 ms) have been used, according to the discharge burning particularity. Also, it affects the parameters determination accuracy.

Temperature of excited hydrogen electron population levels is determined by the relative intensities (two lines of 656 nm and 486 nm). For the case where the working liquid is distilled water -  $T_e^*(H) = 5500 \pm 700$  K ( $I = 300$  mA,  $U = 1.9-2.4$  kV, air flow - 27.5, 55 and 82.5  $cm^3/s$ , the flow of  $CO_2$  - 4.25, 8.5, 17, 42.5 and 85  $cm^3/s$ ) and as for the bioethanol  $T_e^*(H) = 6000 \pm 500$  K - ( $I = 300$  mA,  $U = 2 - 2.2$  kV, air flow - 55 and 82.5  $cm^3/s$ , the flow of  $CO_2$  - 4.25, 8.5 and 17  $cm^3/s$ ). Also, the oxygen  $T_e^*(O)$  has been defined by the Boltzmann diagrams method, in the case of distilled water. The three most intense lines (777.2 nm, 844 nm, 926 nm) are used in this method. So, we have  $T_e^*(O) = 4700 \pm 700$  K.

Temperatures of OH excited vibrate and rotational population levels have been determined by comparing the experimentally measured emission spectra with the molecular spectra modeled in The SPECAIR program. In the case when the working liquid is distilled water, appropriate temperatures are:  $T_r^*(OH) = 3000 \pm 1000$  K,  $T_v^*(OH) = 4000 \pm 1000$  K ( $I = 300$  mA,

$U = 1.9\text{--}2.4$  kV, air flow - 27.5, 55 and 82.5 cm<sup>3</sup>/s, the flow of CO<sub>2</sub> - 4.25, 8.5, 17, 42.5 and 85 cm<sup>3</sup>/s). Also, population temperatures of vibration and rotational levels for OH and CN have been determined in case of C<sub>2</sub>N<sub>5</sub>ON/H<sub>2</sub>O (1/9.5) solution as the working liquid, they are:  $T_r^*$  (OH) = 3500 ± 500 K,  $T_v^*$ (OH) = 4000 ± 500 K,  $T_r^*$ (CN) = 4000 ± 500 K,  $T_v^*$ (CN) = 4500 ± 500 K ( $I = 300$  mA,  $U = 2 - 2.2$  kV, air currents - 55 and 82.5 cm<sup>3</sup>/s, the flow of CO<sub>2</sub> - 4.25, 8.5 and 17 cm<sup>3</sup>/s). Temperatures for other molecular components haven't been determined because of their bands low intensity.

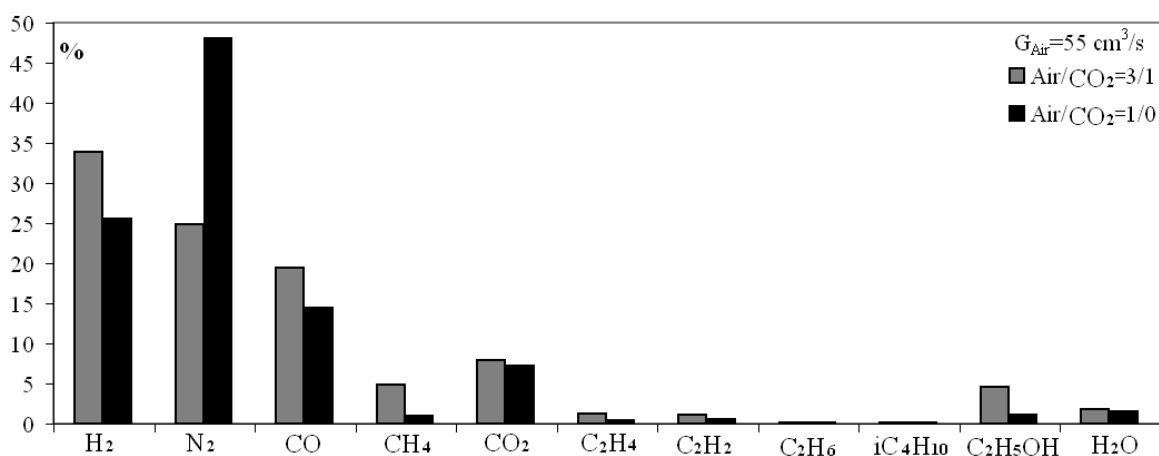
During the study, it turned out that the addition of CO<sub>2</sub> weakly affects the population temperature of excited electron, vibration and rotational levels of plasma components (Fig. 5) ( $I = 300$  mA,  $U = 1.9 - 2.4$  kV, air flow - 27.5, 55 and 82.5 cm<sup>3</sup>/s, the flow of CO<sub>2</sub> - 4.25, 8.5, 17, 42.5 and 85 cm<sup>3</sup>/s). Weak tendency to temperature decrease has been observed, but these changes do not exceed the error.



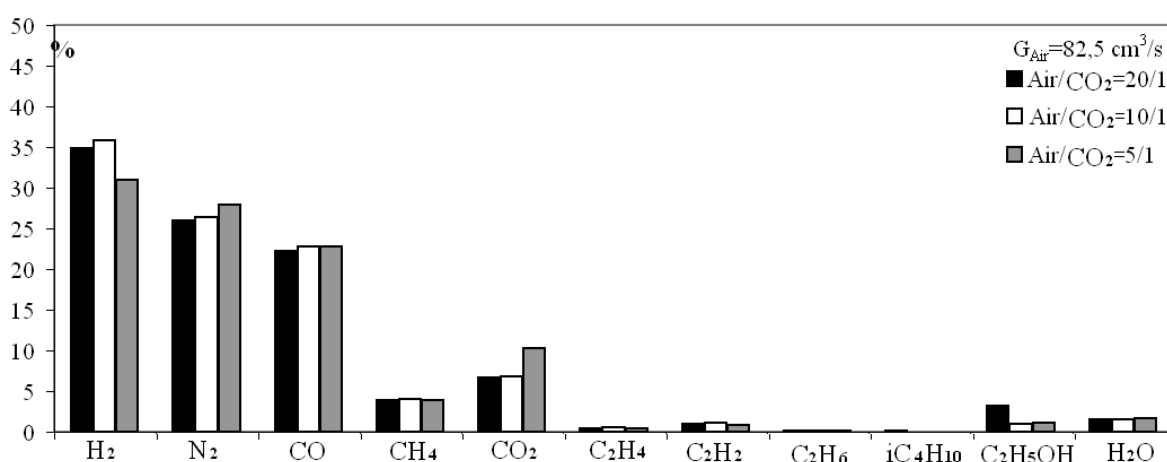
**Figure 5.** Population temperatures of excited electron, vibration and rotational levels of plasma components at different ratio of CO<sub>2</sub>/Air in the working gas. Working liquids - distilled water (a) and ethanol (b)

Fig. 6–7. shows the results of gas chromatography bioethanol conversion output products. Results are presented for two air streams 55 and 82.5 cm<sup>3</sup>/s + three CO<sub>2</sub> streams: 4.25, 8.5 and 17 cm<sup>3</sup>/s ( $I = 300$  mA,  $U = 2 - 2.2$  kV). CO<sub>2</sub>/Air ratio in the range from 1/20 to 1/3 has been changing exactly this way. Selection of gas into the flask has been taken place at the refrigerator output. The flask has been previously pumped by the water-jet pump to the pressure of saturated water vapor (23 mm Hg).

Fig. 6 shows the gas chromatography comparison of bioethanol conversion output products with and without the addition of CO<sub>2</sub>. The air flow is constant – 55 cm<sup>3</sup>/s, in case of CO<sub>2</sub>/Air = 1/3 – 17 cm<sup>3</sup>/s of CO<sub>2</sub> has been added to the air (the total flow has been increased, which may explain the decrease in the percentage of nitrogen at a constant air flow;  $I = 300$  mA,  $U = 2 - 2.2$  kV). This histogram shows that adding of carbon dioxide leads to a significant increase of the H<sub>2</sub> component percentage, CO (syn-gas) and CH<sub>4</sub> in the output gas. This may indicate that the addition of CO<sub>2</sub> during the ethanol reforming increases the conversion efficiency, because CO<sub>2</sub> plays a burning retarder role.



**Figure 6.** Gas chromatography comparison of bioethanol conversion output products with and without the addition of CO<sub>2</sub>.

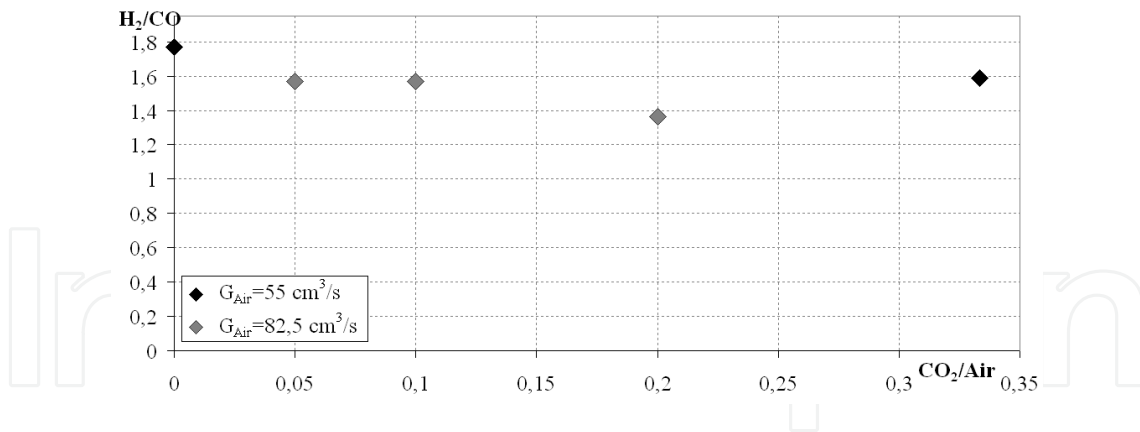


**Figure 7.** Gas chromatography comparison of bioethanol conversion output products by adding different amounts of CO<sub>2</sub>.

The ethanol solution consumption for the SC mode with current of 300 mA and air flow of 55 cm<sup>3</sup>/s equals 6 ml/min, and for the air flow of 82.5 cm<sup>3</sup>/s and CO<sub>2</sub> of 17 cm<sup>3</sup>/s mixture - 10 ml/min.

According to the gas chromatography, in the studied correlations range of CO<sub>2</sub>/Air, syn-gas ratio ([H<sub>2</sub>]/[CO]), changes slightly – look at Fig. 8. Measurements were made by two air streams of 55 and 82.5 cm<sup>3</sup>/s and three CO<sub>2</sub> streams of – 4.25, 8.5 and 17 cm<sup>3</sup>/s; I = 300 mA, U = 2 – 2.2 kV.

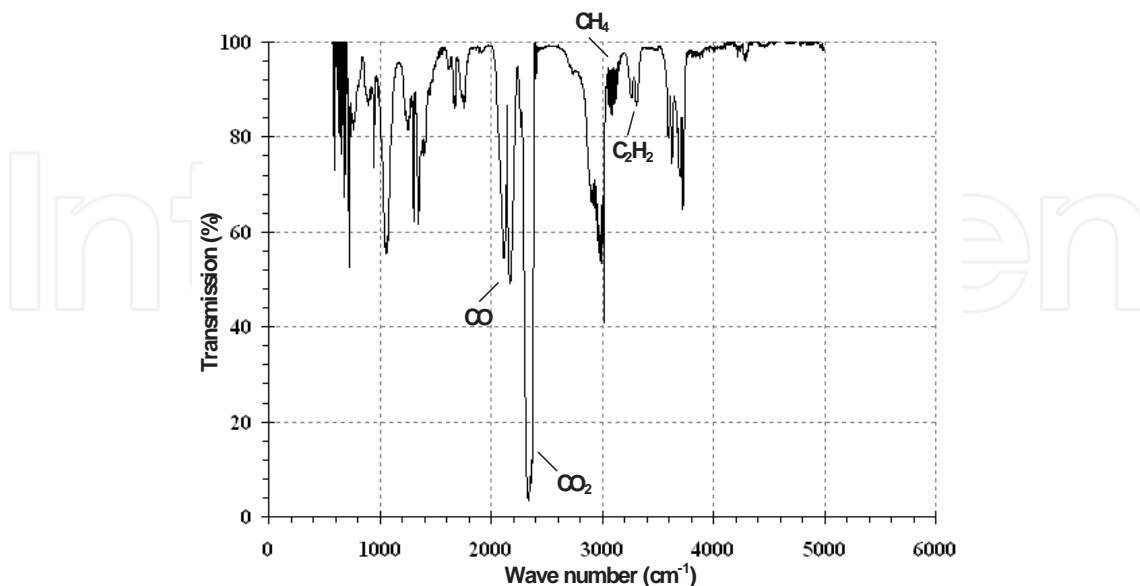
Besides the gas chromatography, the output gas composition has been studied by means of infrared spectrophotometry (IRS). Fig. 9 shows a typical IRS spectrum of the output gas. In the SC mode (current 300 mA, voltage 2 kV) the working liquid is ethyl alcohol and distilled water mixture (C<sub>2</sub>H<sub>5</sub>OH/H<sub>2</sub>O = 1/9.5), and the working gas – air (82.5 cm<sup>3</sup>/s) and CO<sub>2</sub> (4.25 cm<sup>3</sup>/s) mixture. Research has been carried out in a ditch with a length of 10 cm and a diameter of 4 cm. Pressure inside the ditch has been 1 atm. The ditch walls have been made of BaF<sub>2</sub>.



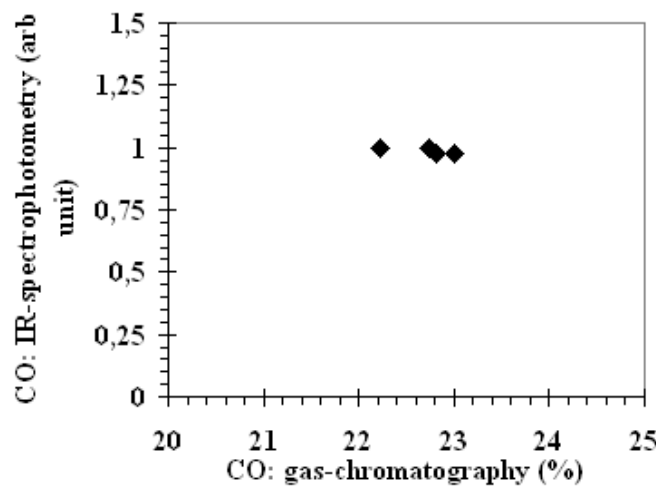
**Figure 8.** Syn-gas ratio of bioethanol conversion output products for various ratios of CO<sub>2</sub>/Air in the range between 0/1 - 1/3.

Fig. 10 shows the dependence of the CO transmission standardized maximum intensity peaks (2000 - 2250 cm<sup>-1</sup>) in the syn-gas, depending on the CO concentration according to gas chromatography results. Standardization has been conducted for the maximum intensity value of the CO transmission peak bandwidth at the SC mode with the current of 300 mA, voltage - 2 kV, the mixture of ethyl alcohol and distilled water (C<sub>2</sub>H<sub>5</sub>OH/H<sub>2</sub>O = 1/9.5) as the working liquid, and the mixture of air (82.5 cm<sup>3</sup>/s) and CO<sub>2</sub> (4.25 cm<sup>3</sup>/s), as the working gas.

According to IR spectrophotometry CO fraction in the synthesis gas is practically the same. According to gas chromatography CO fraction in the synthesis gas in the different operation modes stays on the same level as well (the changes are in the range of 1%). So IR spectrophotometry can be used determine the composition of synthesis gas under ethanol reforming.



**Figure 9.** The SC mode (current 300 mA, voltage 2 kV) the working liquid is ethyl alcohol and distilled water mixture (C<sub>2</sub>H<sub>5</sub>OH/H<sub>2</sub>O = 1/9.5), the working gas – air (82.5 cm<sup>3</sup>/s) and CO<sub>2</sub> (4.25 cm<sup>3</sup>/s) mixture



**Figure 10.** Dependence of the normalized maximum intensity peaks (2000-2250  $\text{cm}^{-1}$ ) transmission of CO in the syn-gas, depending on the concentration of CO according to gas chromatography data.

Plasma provides gas generation, which contains a certain amount of the syn-gas. The energy needed for this plasma support ( $Q_p$ ) has been calculated by the following formula:

$$Q_p = P_d t, \quad (1)$$

where  $P_d$  - power that has been embedded into the discharge,  $t$  - production time of gas volume unit during the reforming process. Electrical energy transformation coefficient  $\alpha$  has been calculated by the formula:

$$\alpha = \frac{Q_s}{Q_p} \quad (2)$$

where  $Q_s$  - energy that is released during the complete combustion of syngas (obtained in the reforming process).

Electrical energy transformation coefficient  $\alpha$  has value of 0.81 for the "TORNADO-LE" with an ethanol solution and pure air flow  $55 \text{ cm}^3/\text{s}$ . And the  $\text{CO}_2$  addition (the ratio of  $\text{CO}_2/\text{air} = 1/3$ ) gives the value of  $\alpha = 1,01$ . System electrical parameters are as follows:  $I = 300 \text{ mA}$ ,  $U = 2 - 2.2 \text{ kV}$ .

### 2.3. Model and calculations

In the model of calculations was assumed that the discharge is homogeneous over the entire volume. It is justified at zero approximation, because the time of gas mixing in the radial direction is less than the times of characteristic chemical reactions. Also we neglect the processes in the transitive zone between the discharge to post-discharge. Thus, the time of gas

pumping through the transition region is too short for the chemical reactions to have a sufficient influence on the concentration of neutral components.

The total time of calculation is divided into two time intervals: the first one is the calculation of the kinetic processes of fast generation of active atoms and radicals in the discharge region. Those components accelerate the formation of molecular hydrogen, carbon oxides and production of other hydrocarbons. The second time interval is the oxidation of the gas mixture in the post-discharge region as a result of the high gas temperature and the presence of O and OH. These components remain in the mixture after the dissociation of water and oxygen molecules by electron impacts in the plasma. The oxidation of generated hydrocarbons has a noticeable influence on kinetics in the investigated mixture due to the high gas temperature.

Under the aforementioned conditions, the characteristic time of oxidation is approximately equal to the air pumping time through the discharge region ( $\sim 10^{-3}$ – $10^{-2}$  s). The following system of kinetic equations is used in order to account for the constant air pumping through the system:

$$\frac{dN_i}{dt} = S_{ei} + \sum_j k_{ij} N_j + \sum_{j,l} k_{ijl} N_j N_l + \dots + K_i - \frac{G}{V} N_i - kN_i \quad (3)$$

$N_i$ ,  $N_j$ ,  $N_l$  in the equation (3) are the concentrations of molecules and radicals;  $k_{ij}$ ,  $k_{ijl}$  are the rate constants of the processes for the  $i$ -th component. The rates of electron–molecule reactions  $S_{ei}$  are connected with discharge power and discharge volume. The last three terms in equation (1) describe the constant inflow and outflow of gas from the discharge region. The term  $K_i$  is the inflow of molecules of the primary components (nitrogen, oxygen, carbon dioxide, water and ethanol) into the plasma,  $G/VN_i$  and  $kN_i$  are the gas outflow as the result of air pumping and the pressure difference between the discharge region and the atmosphere. In order to define the initial conditions, the ethanol/water solution is assumed to be an ideal solution. Therefore, the vapor concentrations are linear functions of the ethanol-to-water ratio in the liquid. The evaporation rates  $K_i$  of  $C_2H_5OH$  and  $H_2O$  are calculated from the measured liquids' consumption. The inflow rates  $K_i$  of nitrogen and oxygen are calculated by the rate of air pumping through the discharge region:

$$K_i = \frac{G}{V} N_i^0 \quad (4)$$

where  $N_i^0$  correspond to  $[N_2]$  and  $[O_2]$  in the atmospheric pressure air flow.

The gas temperature in the discharge region is taken to be constant in the model. In reality, the gas temperature  $T$  is dependent on the gas pumping rate and the heat exchange with the environment. Therefore, in order to take into account those influences,  $T$  is varied in the interval 800–2500K (similarly to the experimentally obtained temperature spread). After  $\sim 10^{-2}$  s, the balance between the generation and decomposition of the components leads to saturation

of concentrations of all species. This allows us to stop the calculations in the discharge region and to investigate the kinetics in the post-discharge region. System (3) is solved without accounting for the last three terms on the time interval without the plasma. The calculations are terminated when the molecular oxygen concentration reaches zero level.

The full mechanism developed for this experimental work is composed of 30 components and 130 chemical reactions between them and its closed to [11]. The charged particles (electrons and ions) are ignored in the mechanism, because of low degree of ionization of the gas ( $\sim 10^{-6} - 10^{-5}$ ). Nitrogen acts as the third body in the recombination and thermal dissociation reactions. In the non-equilibrium plasma almost the entire energy is deposited into the electron component. The active species, generated in the electron-molecular processes, lead to chain reactions with ethanol molecules.

Numerical simulation of kinetics showed that the main channels of  $H_2$  generation in the plasma were ethanol abstraction for the first  $10-100\mu s$ , and hydrocarbon abstraction afterwards. Additionally, the conditions when the reaction between  $H_2O$  and hydrogen atoms was the main channel of  $H_2$  production were found. A kinetic mechanism, which adequately described the chemistry of the main components, was proposed. The model did not account for nitrogen-containing species, and nitrogen was considered only as a third body in recombination and dissociation reactions. The comparison between experiments and calculations showed that the mechanism can adequately describe the concentrations of the main components ( $H_2$ ,  $CO$ ,  $CO_2$ ,  $CH_4$ ,  $C_2H_4$ ,  $C_2H_6$ , and  $C_2H_2$ ).

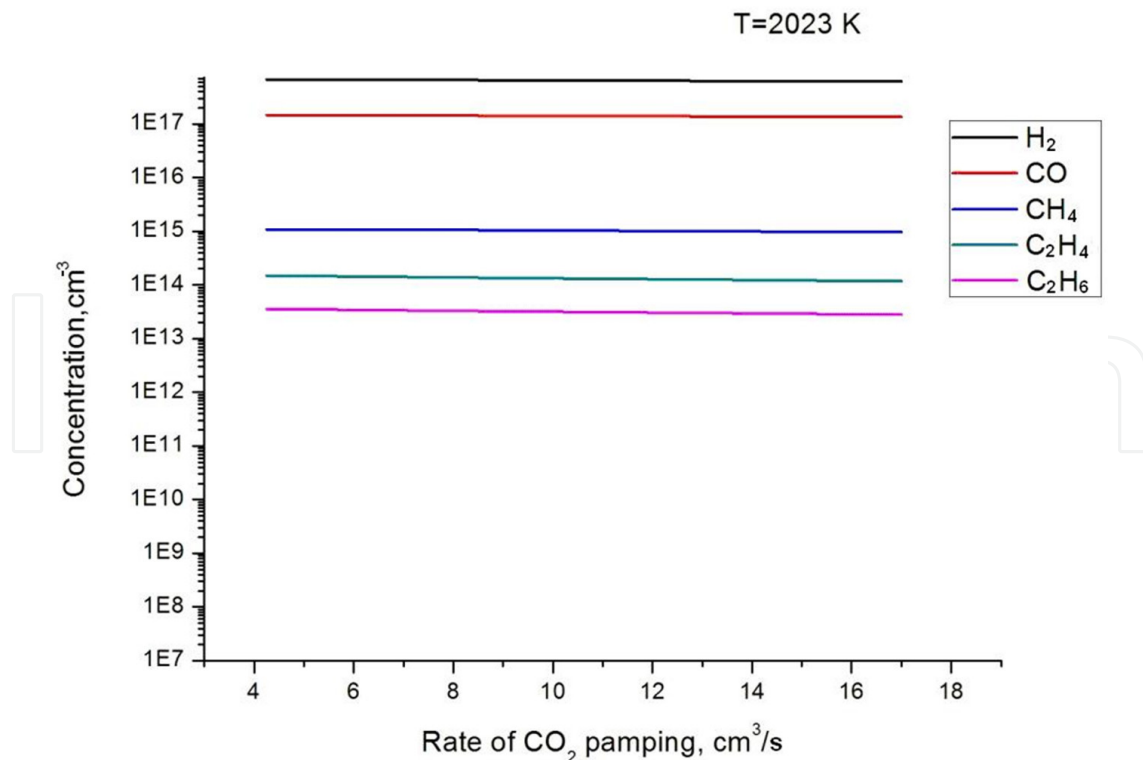
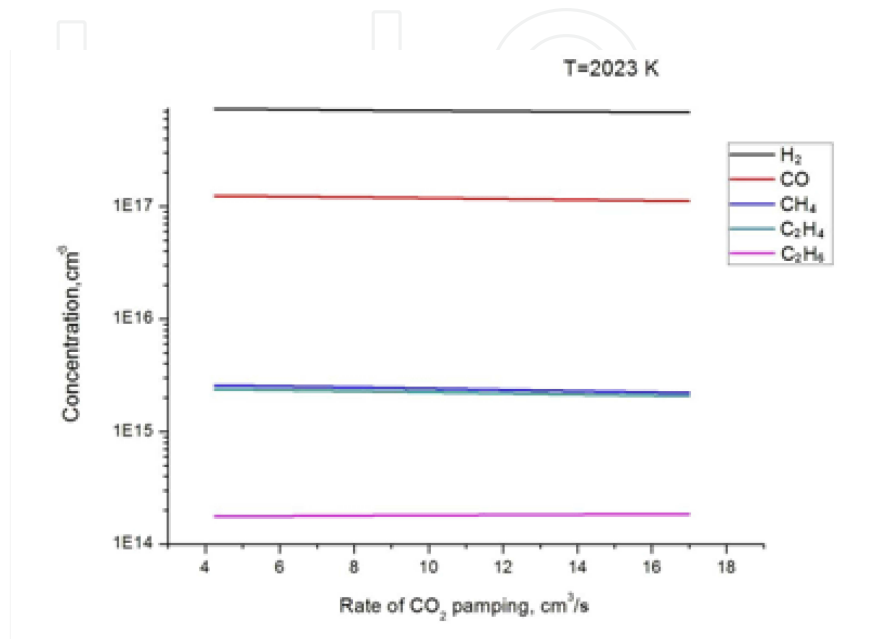


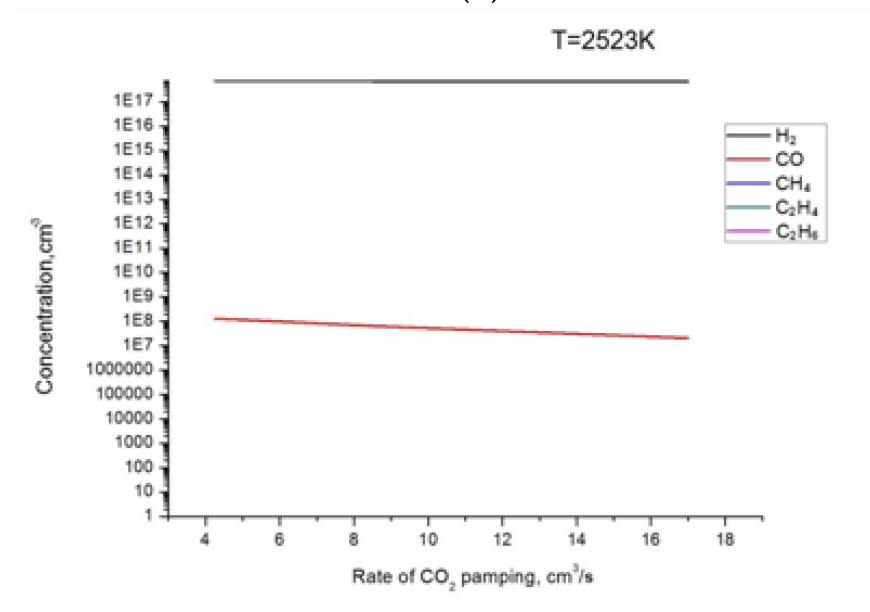
**Figure 11.** The dependence of the reaction main products of the flow rate of  $CO_2$  (inside discharge),  $T = 2023\text{ K}$



However, it should be noted that with the increase in temperature to 2523 K leads to the fact that the output of the reactor is not observed almost no light hydrocarbons. They simply "fall apart" and burned. That leaves the most stable elements such as  $\text{H}_2\text{O}$ ,  $\text{N}_2$ ,  $\text{CO}_2$ . This suggests that the increase in temperature up to these values is not advisable because of the decrease in the yield of useful products (see Fig. 11 and Fig. 12a,b).



(a)



(b)

**Figure 12.** a). The dependence of the reaction main products of the flow rate of  $\text{CO}_2$  (after discharge),  $T = 2023\text{ K}$ . b). The dependence of the reaction main products of the flow rate of  $\text{CO}_2$  (after discharge),  $T = 2523\text{ K}$

These calculations are based in good correspondence with the experimental data (see Fig. 8).

Other model hydrocarbon is bioglycerol (crude glycerol) which is a byproduct of the biodiesel manufacture. Biodiesel is a popular alternative fuel. It is carbon neutral, has emissions equivalent or below diesel, is biodegradable, non-toxic, and is significantly cheaper to manufacture than its petroleum equivalent. However there is one significant drawback: for every 10 gallons of biodiesel produced, roughly 1 gallon of bioglycerol is created as a byproduct.

Biodiesel is produced by mixing vegetable oil and potassium hydroxide KOH. Therefore, the large-scale production of environmentally friendly and renewable fuel may lead to possible bioglycerol accumulation in large quantities, which, in turn, can cause environmental problems, as it is comparably bad fuel. In addition, it has a rather large viscosity of  $1.49 \text{ Pa}\cdot\text{s}$ , which is larger for almost three orders of magnitude than ethanol and water viscosity. The solution to this problem would be "TORNADO-LE" usage for bioglycerol reforming. Pure glycerol chemical formula is  $\text{C}_3\text{H}_5(\text{OH})_3$ . However, bioglycerol contains various impurities (including a set of alkali).

Fig. 13 shows a photograph of burning discharge, where the working liquid is bioglycerol and working gas - air. Research is conducted by the SC polarity, because this mode has lowest liquid consumption.

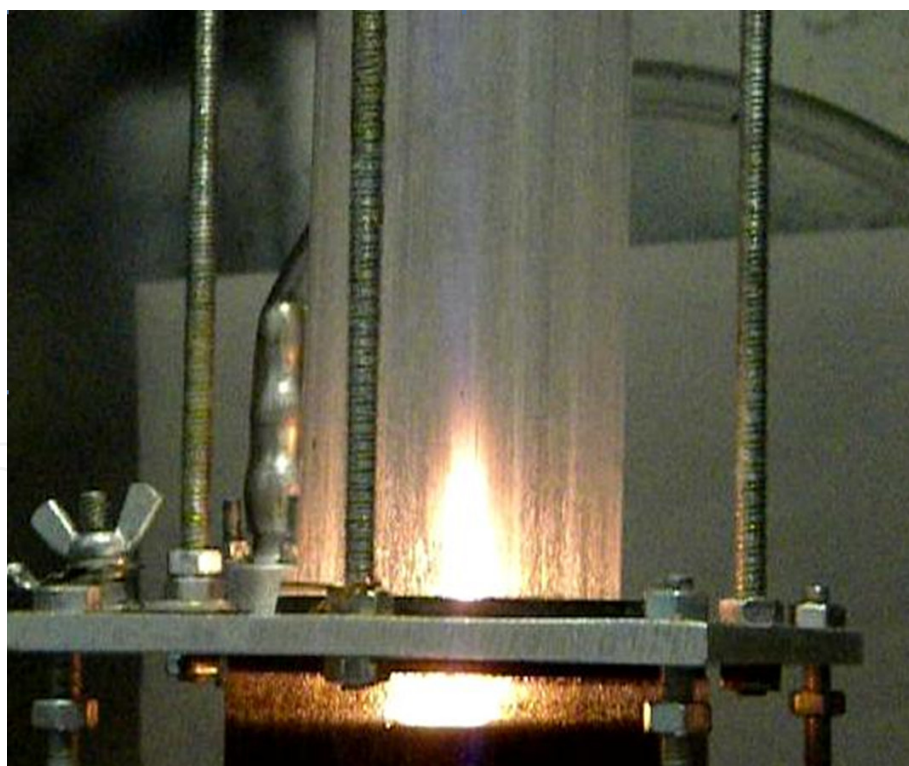


**Figure 13.** Photo of the combustion discharge in which the working liquid is bioglycerol and working gas - air.

Fig. 14 shows the typical emission spectrum of the plasma discharge in a "TORNADO-LE" where the working liquid is bioglycerol doped with alkali. It is registered at a current of 300

mA, voltage – 2 kV, air flow – 110 cm<sup>3</sup>/s. Optical fiber is oriented on the sight line, parallel to the liquid surface in the middle of the discharge gap. The distance from the liquid surface to the top flange equals 10 mm.

Emission spectrum (Fig. 14) is normalized to the maximum Na doublet (588.99 nm, 589.59 nm). It contains K (404.41 nm, 404.72 nm, 766.49 nm, 769.89 nm), Na (588.99 nm, 589.59 nm), Ca (422.6 nm) lines, and a part of continuous spectrum, which indicates that there's a soot in the discharge. Temperature, which is defined by the plasma continuous emission spectrum is  $2700 \pm 100$  K.

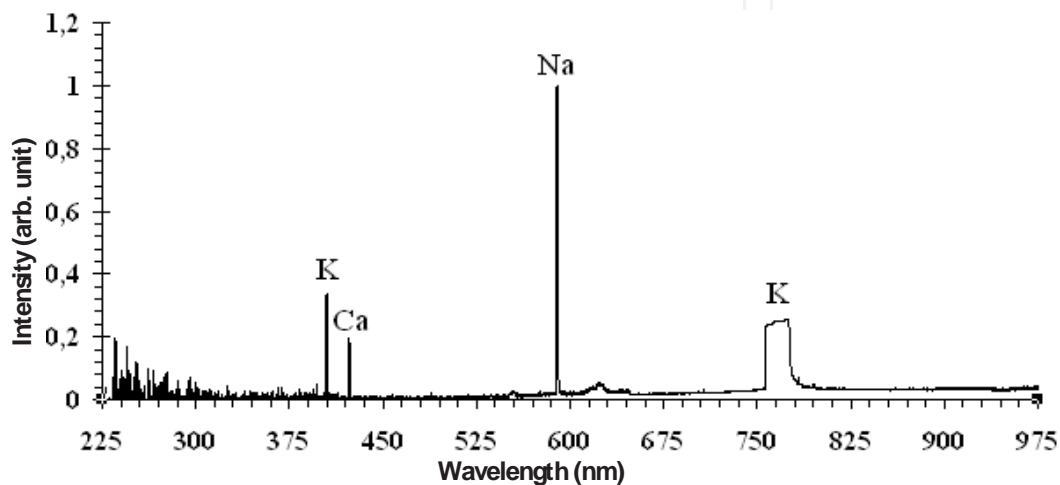


**Figure 14.** Typical emission spectrum of the plasma discharge, which burns in a mixture of air and bioglycerol / alkali.

The K, Na, Ca elements presence in the discharge gap complicates the plasma kinetics numeric modeling of the bioglycerol reform process. The gas flow rate at the system outlet is 190 cm<sup>3</sup>/s, i.e. by 80 cm<sup>3</sup>/s larger than the initial (110 cm<sup>3</sup>/s), which indicates bioglycerol reforming to the syn-gas. Liquid flow is 5 ml/min. Change of the CO<sub>2</sub> share in the working gas weakly affects the spectrum appearance.

Based on the continuous nature of the plasma emission spectra, we compared the experimental results with the calculated spectra of the blackbody radiation. Calculations have been performed by using Planck's formula.

Fig. 15 shows the computational grid with step of 200-300 K in the temperature range from 2500 K to 3500 K and the plasma emission spectrum in the case of bioglycerol, as a working fluid (air flow - 82.5 cm<sup>3</sup>/s, the flow of CO<sub>2</sub> - 17 cm<sup>3</sup>/s, CO<sub>2</sub>/Air = 1/5, I<sub>d</sub> = 300 mA, U = 600 V). All spectra are normalized to the intensity, which is located at a wavelength of 710 nm.

The data in Fig. 15 show that the plasma emission spectrum coincides with the calculated by the Planck formula for the temperature  $T = 2800 \pm 200$  K. Since bioglycerol contains alkali metals, which represent an aggressive environment, the gas chromatography can't be used. Therefore, in order to determine the gas composition, formed the bioglycerol reformation IR and mass spectrometry have been used.

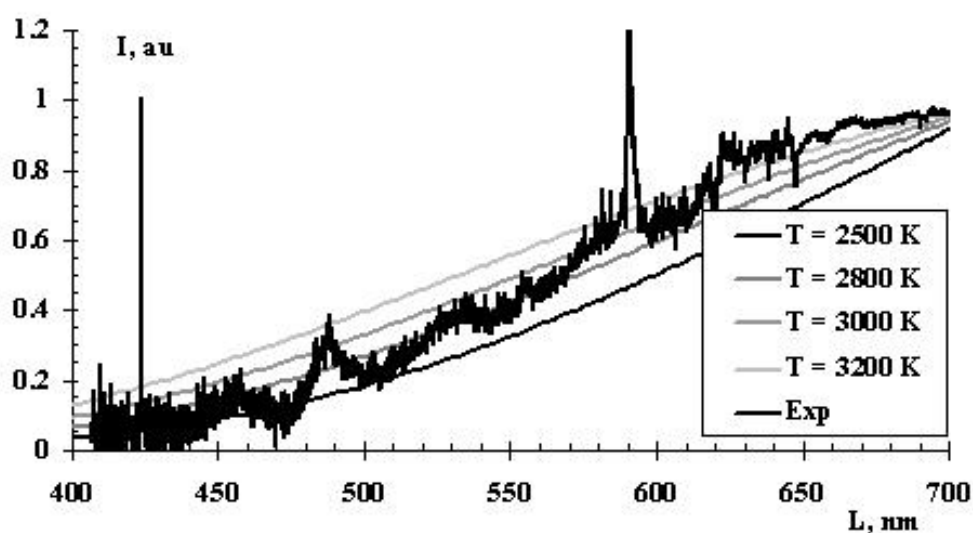


**Figure 15.** Plasma emission spectrum in the case when the working gas is a mixture  $\text{SO}_2/\text{Air} = 1/5$  (air flow - 82.5  $\text{cm}^3/\text{s}$ , the  $\text{CO}_2$  flow - 17  $\text{cm}^3/\text{s}$ ),  $I_d = 300$  mA,  $U = 600$  V and calculated spectra of blackbody radiation)

With infrared transmission spectra one can see that the transition to bioglycerol increases the amount of such components as  $\text{CO}_2$  (2250-2400  $\text{cm}^{-1}$ ),  $\text{CO}$  (2000-2250  $\text{cm}^{-1}$ ),  $\text{CH}_4$  (3025-3200  $\text{cm}^{-1}$ ),  $\text{C}_2\text{H}_2$  (3200-3350  $\text{cm}^{-1}$ ).

## 2.4. Discussions

Electrical energy is added to the "TONADO-LE" plasma-liquid system in the form of plasma power. Plasma acts as a catalyst and thus this power should be controlled. In addition to electric energy for plasma we incorporate hydrocarbon (ethanol or bioglycerol) as an input to the system. These hydrocarbons are raw material for syn-gas generation but they are also a fuel which has some energy associated with it. So, we input some energy to the system (hydrocarbon + electricity) and we get syn-gas, which is potentially a source of energy as well.

Carbon dioxide adding leads to a significant increase the percentage of  $\text{H}_2 + \text{CO}$  (syn-gas) and  $\text{CH}_4$  components in the exhaust. This may indicate that the  $\text{CO}_2$  addition under the ethanol reforming increases the conversion efficiency, because  $\text{CO}_2$  plays a role of the retarder in the system by reducing the intensity of the conversion components combustion.

The transmission spectra of infrared radiation indicate that the exhaust gas obtained by ethanol solution conversion, contains such components as  $\text{CO}$ ,  $\text{CO}_2$ ,  $\text{CH}_4$ ,  $\text{C}_2\text{H}_2$ . It was found that  $\text{CO}_2$  adding reduces the  $\text{CH}_4$  and  $\text{C}_2\text{H}_2$  amount, but does not affect the amount of produced  $\text{CO}$ .

The possibility of hydrocarbons reforming, which have considerable viscosity (bioglycerol) in the "TORNADO-LE" is shown. This gives a possibility to avoid environmental problems due to the bioglycerol accumulation during biodiesel production.

The  $\alpha$  coefficient [see (2)] in bioglycerol reforming is higher than ethanol reforming at the same ratios of  $\text{CO}_2/\text{Air}$  in the input gas. This may be connected with the lower power consumption

on the plasma generation in case of bioglycerol reforming. Bioglycerol contains alkaline ash, which increases the bioglycerol conductivity. Bioglycerol reforming products contain mainly CO and hydrocarbons  $\text{CH}_4$ ,  $\text{C}_2\text{H}_2$ , which also gives some contribution to energy yield.

### 3. Dynamic impulse plasma-liquid systems

#### 3.1. Experimental set up

The experimental setting is shown in Fig. 16. The main part of the system is cylinder with height  $H = 10$  mm, and radius  $R = 135$  mm. Its lateral surface made of stainless steel with a thickness of 5 cm. This cylinder is filled with liquid for experimental operations. The electrodes are placed perpendicular to the cylinder axis. They have the diameter of 10 mm, made of brass, and their ends are shaped hemispheres with a radius of curvature of 5 mm. The discharge (2) is ignited between the rounded ends of the electrodes. At a distance of 40 mm from the lateral surface of the cylinder is piezo-ceramic pressure sensor (3), which records acoustic vibrations in the fluid, caused by electric discharge under water. The distance between the sensor head and the system axis =  $L$ .

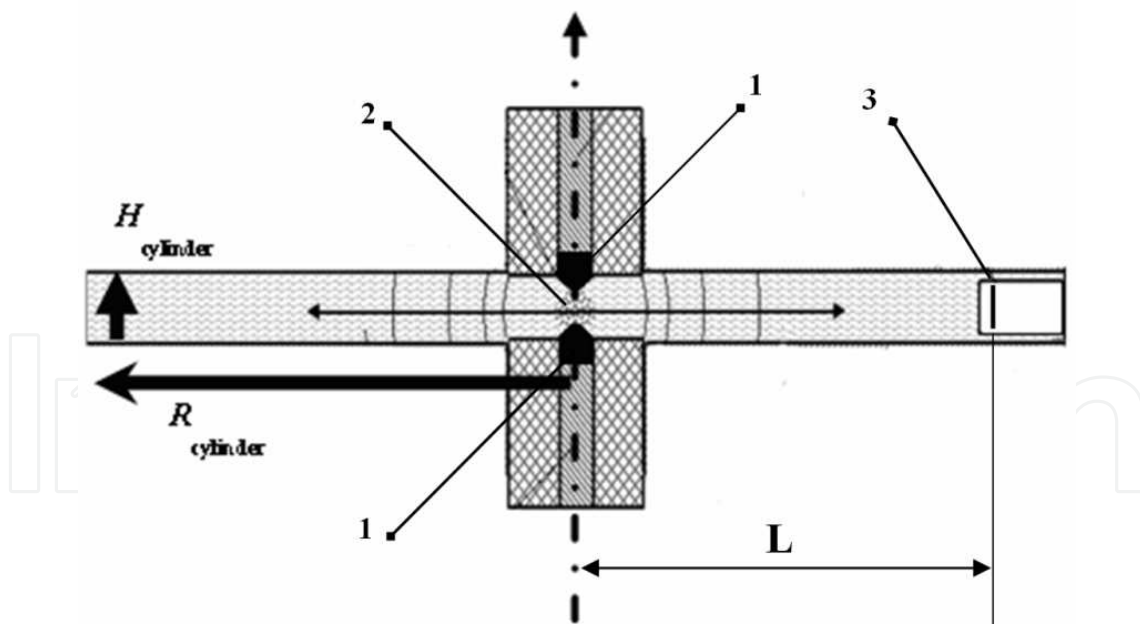


**Figure 16.** Schematic diagram of plasma-liquid system with a pulsed discharge, 1 - electrodes with brass tips, 2 - plasma, 3 - piezo-ceramic pressure sensor.

The cylindrical system could be located in a horizontal position (Fig. 17a) or vertical one (Fig. 17b). The full volume (0.5 l) of system is fluid-filled. The fluid in the system can be processed

as in static mode (no flow), and dynamic one (with flow  $\sim 15 \text{ cm}^3/\text{s}$ ). Additional supply of gas may be realized in the system also (airflow  $\sim 4 \text{ cm}^3/\text{s}$ ), which is injected through a spray nozzle (source diameter 8 mm) located near the inner wall of the cylinder at a distance of 130 mm from the discharge gap (Fig. 16). The working fluids are: the tap water (with and without flow), distillate and ethanol (96%, no flow).

The main feature of electrical scheme for pulsed power feeding of discharge in a liquid is usage of two independent capacitors which are supplied two independent sources of power (1 kW). Pulsed discharge realized in two modes: single and double pulses. In the single pulse mode only one capacitor is discharged with a frequency of 0 - 100 Hz.

Double pulse mode is realized as follows: one capacitor discharges in the interelectrode gap through air spark gap; the clock signal from the Rogowski belt after first breakdown is applied to the thyatron circuit and second capacitor discharges through it. This set of events leads to the second breakdown of the discharge gap and second discharge appearance.

Delay of the second discharge ignition may be changed in range of 50 - 300 microseconds. The following parameters are measured: discharge current and the signal from the pressure sensor. The Rogowski belt has the sensitivity 125 A/V, and its signal is recorded with an oscilloscope. Capacity for the first discharge ( $C_1$ ) = 0.105  $\mu\text{F}$  and it is charged to  $U_1 = 15 \text{ kV}$  (energy  $E_1 = 12 \text{ J}$ ), capacity for the second discharge  $C_2 = 0.105 \mu\text{F}$  and it is charged to  $U_2 = 18 \text{ kV}$  (energy  $E_2 = 17 \text{ J}$ ).

A distance between electrodes can be changed in the range of 0.25 - 1 mm. The second discharge can be ignited at the moment (according to the delay tuning) when the reflected acoustic wave, created by the first electric discharge in liquid, returns to the center of the system (the time of its collapse  $\sim 180 \text{ ms}$ ).

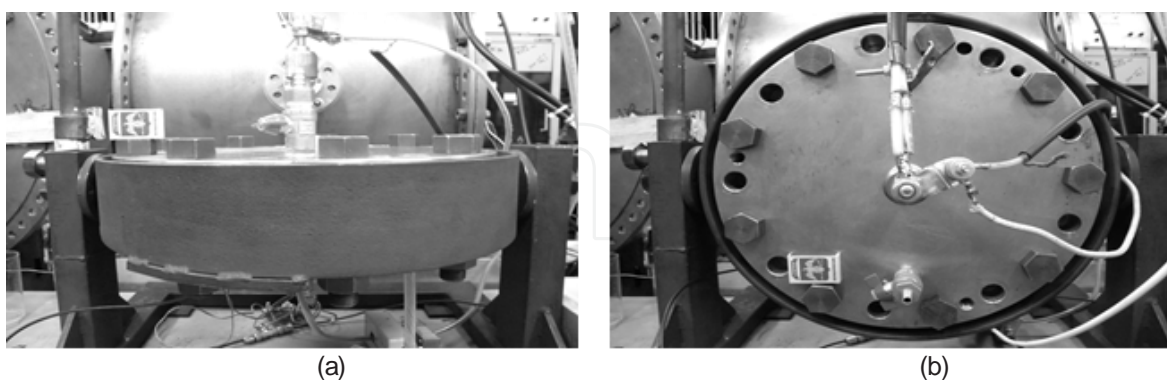


**Figure 17.** Photograph of the cylinder from the outside: a) horizontal position, b) vertical position.

The composition of ethanol and bioethanol reforming products is studied with gas chromatography, in case of bioglycerol reforming - mass spectrometry and infrared spectrophotometry.

### 3.2. Results

Oscillograms of current and acoustic signal for different distances between electrodes (0.5 and 1 mm) are presented in Fig. 18. These oscillograms show the presence of electrolysis phase before breakdown, while duration of electrolysis increases with interelectrode distance.

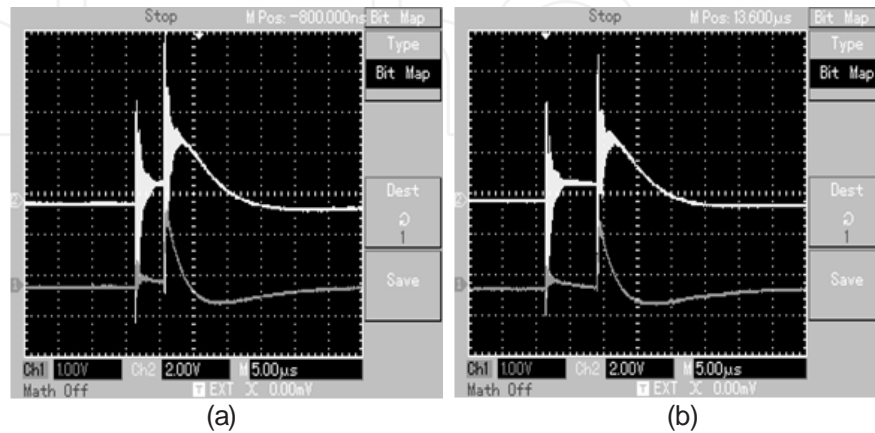


**Figure 18.** Oscillograms of the discharge current (top curve) and signal piezo-ceramic pressure sensor (lower curve): a)  $d = 0.5$  mm, b)  $d = 1$  mm. Tap water flow =  $15 \text{ cm}^3/\text{sec}$ , without the input gas stream,  $C = 0.18 \text{ uF}$ ,  $U = 13.5 \text{ kV}$ ; ballast resistor in the discharge circle:  $R_b = 20 \text{ Ohm}$ , the cylinder is in horizontal position.

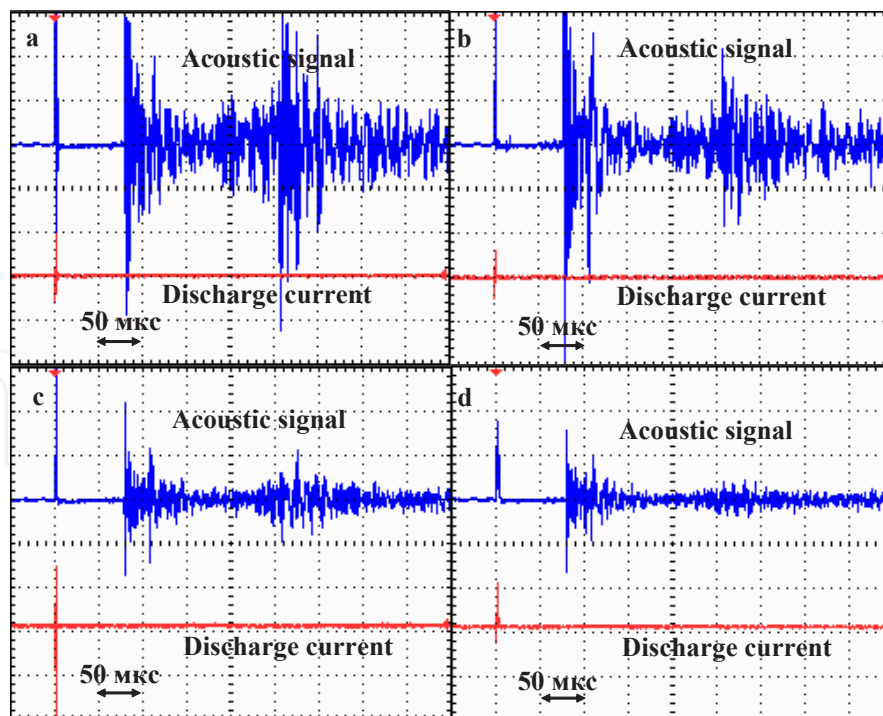


**Figure 19.** Oscillograms of current and acoustic signal in the single pulse mode at the different discharge ballast resistor:  $R_b$ : a) - 0 Ohm, b) - 10 Ohm; c) - 20 Ohm, d) - 50 Ohm. Tap water flow  $15 \text{ cm}^3/\text{s}$ , without the input gas stream,  $d = 0.5$  mm,  $C = 0.015 \text{ uF}$ ,  $U = 19.5 \text{ kV}$ , the cylinder is in horizontal position.

Fig. 19 shows the acoustic signal dependence from ballast resistor in the discharge electric circuit. The acoustic signal has two splashes: №1 - the first diverging acoustic wave, and №2 - the second diverging acoustic wave. When the ballast resistor is increased, first and second acoustic signal splashes are decreased. This may be due to the fact: we increase the ballast resistor and set measures to the discharge current, as a result the injected into the discharge gap energy is diminished.

Also, there is a signal immediately behind the front of the first splash, which is founded in all cases at 110 microseconds interim from the beginning of the discharge current. The acoustic wave passes the way near 17 cm during this time. The pressure sensor is located at the distance of 2 cm from the lateral surface, so the acoustic signal passes the way near 12 cm to the sensor. Thus, there is a second stable signal after the first splash through time  $\sim 29 \mu\text{s}$ , which corresponds to the path  $\sim 4.4 \text{ cm}$ , so the signal can be the convergent acoustic waves reflected from the wall.

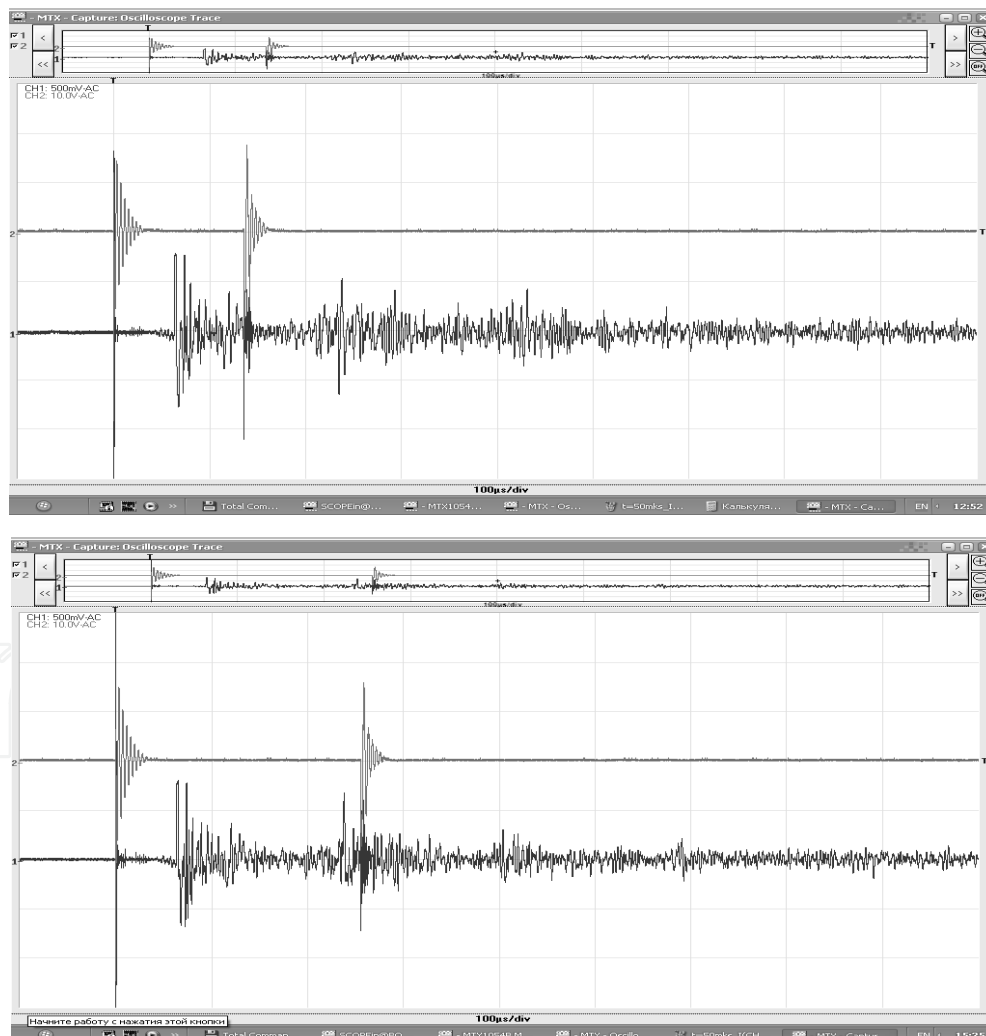


**Figure 20.** Oscillograms of the discharge current (top oscillogram) and acoustic signal (lower oscillogram) at different delays of the second discharge pulse.



There is the third acoustic signal splash in the experiment, but it does not affect the second discharge pulse delay in relation to the first. In addition, there is no acoustic signal from to the second discharge pulse in the double pulse mode, although the single pulse signal is present in the single pulse mode (Fig. 20).

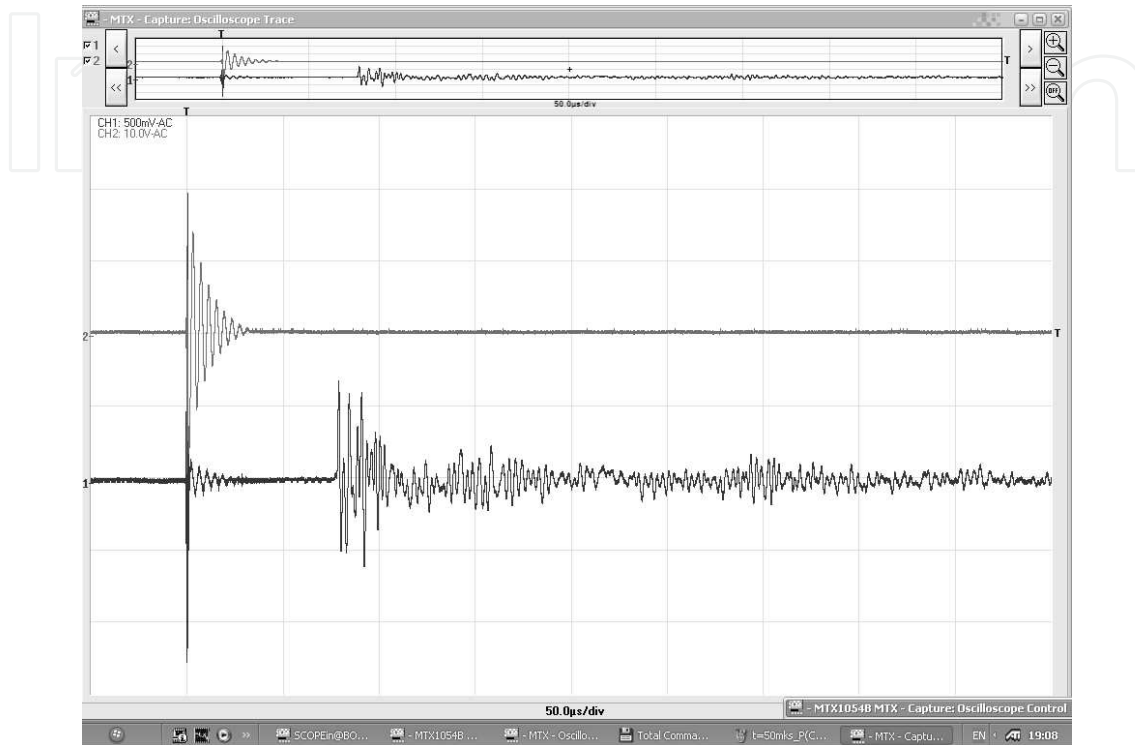


**Figure 21.** Oscillograms of the discharge current (top oscillogram) and the acoustic signal (lower oscillogram) in the single pulses mode. Working fluid - ethanol,  $d = 0.25$  mm,  $C_1 = 0.105$   $\mu$ F,  $U_1 = 15$  kV, the cylinder in the vertical position

Fig. 21 shows clearly that the duration and amplitude parameters for the first current pulse in the ethanol are virtually indistinguishable from the first current pulse in distilled water at any cylinder orientations. The ratio of the second acoustic signal amplitude to the first acoustic signal amplitude in the ethanol is noticeably less than in the tap water and distillate.

The results of oscillographic studies of the discharge current and acoustic signals in double pulses mode demonstrate that the first discharge in double pulses mode takes place in the narrow gas channel with a radius comparable to the size of the plasma channel, and the second discharge takes place in the wide channel with radius larger than the plasma channel.

Next, we present the results of ethanol reforming studies in the impulse plasma-liquid system with double pulses mode and their comparison with the results obtained for "TORNADO-LE".

The mass spectrometer studies of ethanol reforming in the impulse PLS of cylindrical geometry were carried out in the following modes: single pulse mode ( $C = 0.105$   $\mu$ F,  $U = 15$  kV,  $f = 15$  Hz, power 180 W) and double-pulse mode ( $C_1 = C_2 = 0.105$   $\mu$ F,  $U_1 = 15$  kV,  $U_2 = 15$  kV,  $f = 15$  Hz, second pulse delay = 170  $\mu$ s, this time is less on 10  $\mu$ sec than collapse time, the power is 435

Wt), the interelectrode distance - 0.25 mm, working liquid - ethanol (96%), the input airflow is  $4 \text{ cm}^3/\text{s}$ .

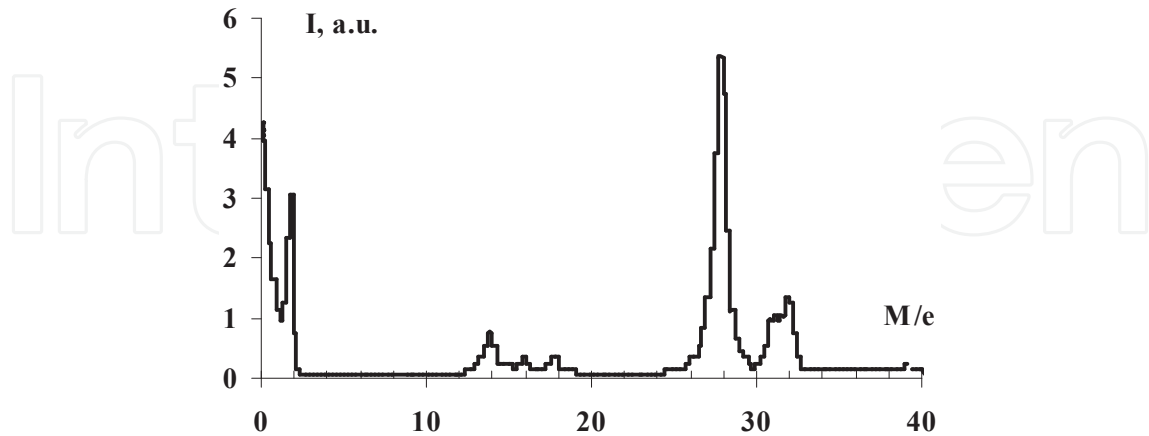


**Figure 22.** Mass spectrum for double pulse mode. Ethanol is without flow, inlet gas stream -  $4 \text{ cm}^3/\text{s}$ ,  $d = 0.25 \text{ mm}$ ,  $C_1 = C_2 = 0.105 \text{ }\mu\text{F}$ ,  $U_1 = 15 \text{ kV}$ ,  $U_2 = 18 \text{ kV}$ , the cylinder is in the vertical position,  $f = 15 \text{ Hz}$ .

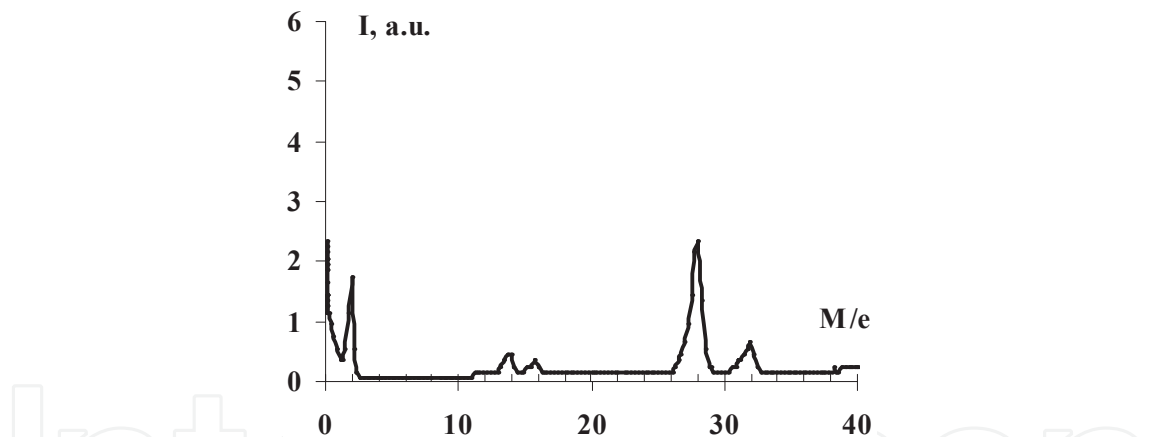


**Figure 23.** Mass spectrum for the single pulse mode. Ethanol without flow, inlet air flow -  $4 \text{ cm}^3/\text{s}$ ,  $d = 0.25 \text{ mm}$ ,  $C_1 = 0.105 \text{ }\mu\text{F}$ ,  $U_1 = 15 \text{ kV}$ , the cylinder is in the vertical position,  $f = 15 \text{ Hz}$ .

The mass spectrometric studies show that the main components of the output fuel mixture are: hydrogen, carbon dioxide, and molecular nitrogen. The values of these components in the mixture:  $\text{H}_2$  - 29%,  $\text{CO}$  - 17% for double pulse mode and  $\text{H}_2$  - 35%,  $\text{CO}$  - 7% for single pulse mode. That is, with the same molecular hydrogen output, the carbon dioxide yield is significantly increased in double pulses mode.

The typical mass spectrum (Fig. 24) of the ethanol reforming (ethanol aqueous solution ethanol with concentrations 3.5, 13 and 26 percents) in the "TORNADO-LE". The power is 640 Wt. It is injected in the plasma for its generation, and inlet air flow is  $55 \text{ cm}^3/\text{s}$ .

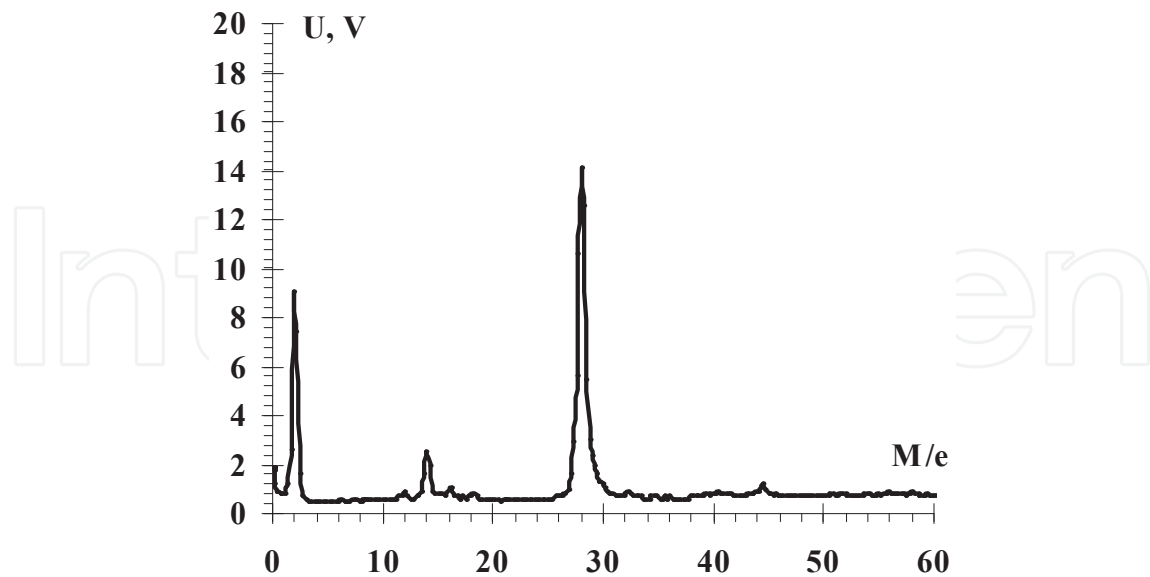


**Figure 24.** Mass spectrum of the output mixture in the ethanol reforming (ethanol - 26%) in "TORNADO-LE" PLS

The following Tab.1 shows the values ratio generating the volume unit of ( $H_2 + CO$ ) mixture per unit of electrical power, which is injected into the plasma under reforming process in the impulse PLS of cylindrical geometry with double pulses mode, and in the "TORNADO-LE":

	Impulse PLS of cylindrical geometry with double pulses mode	"TORNADO-LE"
Single pulse	0.027 cm <sup>3</sup> /Wt	
Double pulses	0.0082 cm <sup>3</sup> /Wt	
Bioethanol 6,5%		0.0024 cm <sup>3</sup> /Wt
Bioethanol 13%		0.0079 cm <sup>3</sup> /Wt
Bioethanol 26%		0.0615 cm <sup>3</sup> /Wt

**Table 1.** The volume unit of ( $H_2 + CO$ ) mixture per unit of electrical power in various PLS

The  $H_2$  and  $CO$  components yield increases with increasing of the ethanol aqueous solution concentration. This concentration has maximum value 26%, and  $H_2$  - 26%,  $CO$  - 14%. The results of these systems studies show, that the pressure, in region collapse of converging shock waves (with pulse energy > 10 J), exceeds critical (Tab. 2). So, the additional increase chemical activity due to supercritical processes inclusion can be achieved in this situation.

Solvent	Molecular mass	Critical temperature, $T_{crit}$	Critical pressure, $P_{crit}$	Critical density, $\rho_{crit}$
	g/mol	K	MPa (bar)	g/sm <sup>3</sup>
CO <sub>2</sub>	44.01	303.9	7.38 (72.8)	0.468
H <sub>2</sub> O	18.015	647.096	22.064 (217.755)	0.322
ethanol	46.07	513.9	6.14 (60.6)	0.276

**Table 2.** Critical parameters of different solvents

## 4. Discussion

The presence of electrolysis phase preceding electrical breakdown of heterophase environment demonstrates that the discharge development in the liquid perform with microbubbles. This result confirms the theory of "bubble" breakdown proposed by Mark Kushner [12].

The formation of convergent acoustic wave after reflection from the ideal solid cylindrical surface was investigated. It is shown that acoustic waves may be effectively focused during these waves passage inside the system.

The research of ethanol reforming in pulse plasma-liquid system has shown that transition from single pulse mode to double pulse mode is accompanied by reduction syn-gase ratio ( $[H_2]/[CO]$ ).

When the working fluid is bioglycerol the K, Na, Ca lines are presented in emission spectra and there is a solid continuous spectrum, which indicates that microparticles are present in the discharge. Its temperature is  $T = 2800 \pm 200$  K.

## 5. General conclusions

On the base of our results in bioethanol and bioglycerol CO<sub>2</sub>-reforming by "TORNADO-LE" plasma-liquid system, we can say that:

1. This process has special features, connected with CO<sub>2</sub> retarding role in the conversion components combustion;
2. In this system there is the possibility of reforming of hydrocarbons with significant viscosity (such as bioglycerol);
3. All the diagnostic methods, used in the "TORNADO-LE" plasma-liquid system, indicate that there're no NO<sub>x</sub> compounds in the bioethanol and bioglycerol reforming products.

The investigations of bioethanol and bioglycerol in pulse plasma-liquid system have shown:

1. The main components of the output fuel mixture in this case are: hydrogen, carbon dioxide, and molecular nitrogen, but the carbon dioxide yield is significantly increased in double pulses mode;
2. The formation of supercritical water in such system and its possible applications for recycling of organic waste and for nanocrystalline particles (in particular, oxide catalysts and other nanocrystalline materials, such as nanotubes) productions needs for additional researches.

## Author details

Valeriy Chernyak<sup>1\*</sup>, Oleg Nedybaliuk<sup>1</sup>, Sergei Sidoruk<sup>1</sup>, Vitalij Yukhymenko<sup>1</sup>, Eugen Martysh<sup>1</sup>, Olena Solomenko<sup>1</sup>, Yulia Veremij<sup>1</sup>, Dmitry Levko<sup>2,3</sup>, Alexandr Tsimbaliuk<sup>2</sup>, Leonid Simonchik<sup>4</sup>, Andrej Kirilov<sup>4</sup>, Oleg Fedorovich<sup>5</sup>, Anatolij Liptuga<sup>6</sup>, Valentina Demchina<sup>7</sup> and Semen Dragnev<sup>8</sup>

\*Address all correspondence to: chernyak\_v@ukr.net

1 Taras Shevchenko National University of Kyiv, Ukraine

2 Institute of Physics, National Academy of Sciences of Ukraine, Kyiv, Ukraine

3 Physics Department, Technion, 32000, Haifa, Israel

4 B.I. Stepanov Institute of Physics, National Academy of Sciences, Minsk, Belarus

5 Institute of Nuclear Research, National Academy of Sciences of Ukraine, Kyiv, Ukraine

6 V.E.Lashkaryov Institute of Semiconductor Physics, National Academy of Science of Ukraine, Kyiv, Ukraine

7 The Gas Institute, National Academy of Science of Ukraine, Kyiv, Ukraine

8 National University of Life and Environmental Sciences of Ukraine, Kyiv, Ukraine

## References

- [1] AEO2011 Early Release Overview, available on the sight: [www.eia.gov/forecast/aeo/pdf/0383er\(2011\).pdf](http://www.eia.gov/forecast/aeo/pdf/0383er(2011).pdf)
- [2] Sharvin E.A., Aristova Ye. Yu., Syn-gas generator for internal combustion engines, "Alternative energy and ecology" (in Russian), 8 (88) 2010, c.31-37

- [3] Nedybaliuk O.A., Chernyak V.Ya., Olszewskij S.V., Plasma-liquid system with reverse vortex flow of "tornado" type (Tornado-LE) //Problems of atomic science and technology, № 6. Series: Plasma Physics (16), p. 135-137. (2010).
- [4] Xumei Tao, Meigui Bai, Xiang Li, e.a., CH<sub>4</sub>-CO<sub>2</sub> reforming by plasma – challenges and opportunities // Progr. in Energy and Combustion Science 37, №2, pp. 113-124, 2011
- [5] V. Chernyak, Eu. Martysh, S. Olszewski, D. Levko. e.a., Ethanol Reforming in the Dynamic Plasma - Liquid Systems, Biofuel Production-Recent Developments and Prospects, Marco Aurélio dos Santos Bernardes (Ed.), (2011). ISBN: 978-953-307-478-8, InTech, P.101-136.
- [6] Lukes, P.; Sunka, P.; Hoffer, P.; Stelmashuk, V.; Benes, J.; e.a.,Book of Abstracts: NATO Science Advanced Research Workshop on Plasma for bio decontamination, medicine and food security, Jasná, Slovakia, March 15–18, 2011.
- [7] Sheldon R. A. C. Catalytic conversions in water and supercritical carbon dioxide from the standpoint of sustainable development (in Russian) // Rus. Chem. J., 48(2004), 74-83.
- [8] N.A.Popov, V.A. Shcherbakov, e.a. Thermonuclear fusion by exploding a spherical charge (gas-dynamical thermonuclear fusion problem) // Uspekhi, 10 (2008), 1087-1094.
- [9] Laux, C.O. Optical diagnostics of atmospheric pressure air plasma SPECAIR / C.O. Laux, T.G. Spence, C.H. Kruger, and R.N.Zare // Plasma Source Sci. Technol. – 2003. - Vol. 12, No. 2. - P. 125-138.
- [10] Raizer Yu.P. Gas discharge physics (Springer, 1991)
- [11] D. Levko, A. Shchedrin, V. Chernyak e.a., Plasma kinetics in ethanol/water/air mixture in a 'tornado'-type electrical discharge // J. Phys. D: Appl. Phys. 44 (2011) 145206 (13pp)
- [12] Kushner, M.J.; Babaeva, N.Yu. Plasma production in liquids: bubble and electronic mechanism, Bulletin of the APS GES10, Paris, France, October 4–8, 2010.

